

AD-A242 107



DTIC

SELECTE

NOV 1 1991

C

D

AD

2

TECHNICAL REPORT ARCCB-TR-91021

EFFECT OF ELEVATED TEMPERATURE TENSILE TESTING OF AF1410 STEEL

E. TROIANO
D. PEEK
E. NIPPES

JUNE 1991



US ARMY ARMAMENT RESEARCH,
DEVELOPMENT AND ENGINEERING CENTER
CLOSE COMBAT ARMAMENTS CENTER
BENÉT LABORATORIES
WATERVLIET, N.Y. 12189-4050



APPROVED FOR PUBLIC RELEASE; DISTRIBUTION UNLIMITED

91 10 31 1 35

91-14764



DISCLAIMER

The findings in this report are not to be construed as an official Department of the Army position unless so designated by other authorized documents.

The use of trade name(s) and/or manufacturer(s) does not constitute an official indorsement or approval.

DESTRUCTION NOTICE

For classified documents, follow the procedures in DoD 5200.22-M, Industrial Security Manual, Section II-19 or DoD 5200.1-R, Information Security Program Regulation, Chapter IX.

For unclassified, limited documents, destroy by any method that will prevent disclosure of contents or reconstruction of the document.

For unclassified, unlimited documents, destroy when the report is no longer needed. Do not return it to the originator.

REPORT DOCUMENTATION PAGE		READ INSTRUCTIONS BEFORE COMPLETING FORM
1. REPORT NUMBER ARCCB-TR-91021	2. GOVT ACCESSION NO.	3. RECIPIENT'S CATALOG NUMBER
4. TITLE (and Subtitle) EFFECT OF ELEVATED TEMPERATURE TENSILE TESTING OF AF1410 STEEL		5. TYPE OF REPORT & PERIOD COVERED Final
		6. PERFORMING ORG. REPORT NUMBER
7. AUTHOR(s) E. Troiano, D. Peek, and E. Nippes (See Reverse)		8. CONTRACT OR GRANT NUMBER(s)
9. PERFORMING ORGANIZATION NAME AND ADDRESS U.S. Army ARDEC Benet Laboratories, SMCAR-CCB-TL Watervliet, NY 12189-4050		10. PROGRAM ELEMENT, PROJECT, TASK AREA & WORK UNIT NUMBERS AMCMS No. 6126.23.1BLO.0AF PRON No. 1A72Z5NHNMSC
11. CONTROLLING OFFICE NAME AND ADDRESS U.S. Army ARDEC Close Combat Armaments Center Picatinny Arsenal, NJ 07806-5000		12. REPORT DATE June 1991
		13. NUMBER OF PAGES 70
14. MONITORING AGENCY NAME & ADDRESS (if different from Controlling Office)		15. SECURITY CLASS. (of this report) UNCLASSIFIED
		15a. DECLASSIFICATION DOWNGRADING SCHEDULE
16. DISTRIBUTION STATEMENT (of this Report) Approved for public release; distribution unlimited.		
17. DISTRIBUTION STATEMENT (of the abstract entered in Block 20, if different from Report)		
18. SUPPLEMENTARY NOTES		
19. KEY WORDS (Continue on reverse side if necessary and identify by block number) Tensile Testing Mechanical Properties Steel Thermal Transients Stress Relaxation		
20. ABSTRACT (Continue on reverse side if necessary and identify by block number) The effect of thermal and mechanical transients on the material properties of AF1410 steel for applications in large caliber ballistic weapons was investigated. The Gleeble Model 1500 thermomechanical simulation device was used for the evaluation of elevated-temperature mechanical properties and simulated firing cycles. The tensile properties and the age-hardening response were measured, as a function of temperature, for one heat of AF1410 steel. (CONT'D ON REVERSE)		

7. AUTHORS (CONT'D)

D. Peek and E. Nippes
Materials Engineering Department
Rensselaer Polytechnic Institute
Troy, NY 12180-3590

20. ABSTRACT (CONT'D)

The results of the investigation showed that the ultimate tensile strength, yield strength, and true fracture stress decreased linearly with increasing temperature, up to 800°F. Young's modulus decreased with increasing temperature, while Poisson's ratio remained unchanged. The material exhibited stress relaxation at elevated temperatures, but not at room temperature, when loaded to 80% of its yield strength. It was found that the yield strength increased when the material had been previously aged at the same temperature.

The age-hardening response of the material exhibited a secondary hardening peak at approximately 900°F. The room-temperature hardness increased with increasing aging temperature up to the secondary hardening peak. A rapid decrease in the room-temperature hardness with increasing aging time occurred at 1000°F.

UNCLASSIFIED

CONTENTS

	Page
LIST OF TABLES	ii
LIST OF FIGURES	iii
ABSTRACT	v
1. INTRODUCTION	1
2. MATERIALS AND PROCEDURE	3
A. Characterization Of Base Material	3
B. Tensile Testing	9
C. Age-Hardening Response Testing	17
D. Metallography	18
3. RESULTS AND DISCUSSION	20
A. Evaluation Of Tensile Tests	20
B. Evaluation Of Age-Hardening Response Tests	38
4. CONCLUSIONS	50
5. LITERATURE CITED	53
7. APPENDIX	55

Accession For	
NTIS GRA&I	✓
DTIC Tab	
Gaining New	
Justification	
By	
Distribution/	
Availability Codes	
Avail and/or	
Dist	Special
A-1	

LIST OF TABLES

	Page
Table 2.1 Chemical Analysis Of AF1410 Steel Used In This Investigation (in weight percent) ...	4
Table 2.2 Fundamental Room-Temperature Mechanical Properties Of AF1410 Steel Used In This Investigation	6
Table 3.1 Tensile Properties For The Longitudinal Orientation Of AF1410 Steel	21
Table 3.2 Tensile Properties For The Transverse Orientation Of AF1410 Steel	22
Table 3.3 Young's Modulus For The Longitudinal Orientation Of AF1410 Steel	29
Table 3.4 Young's Modulus For The Transverse Orientation Of AF1410 Steel	30
Table 3.5 Stress Relaxation After One Hour For The Longitudinal Orientation Of AF1410 Steel .	35
Table 3.6 Stress Relaxation After One Hour For The Transverse Orientation Of AF1410 Steel ...	36
Table 3.7 Tensile Properties For The Longitudinal Orientation Of AF1410 That Were Previously Stress Relaxed At The Same Test Temperature	39
Table 3.8 Tensile Properties For The Transverse Orientation Of AF1410 That Were Previously Stress Relaxed At The Same Test Temperature	40
Table 3.9 The Effects Of Aging Temperature And Aging Time On The Macrohardness Of AF1410 Steel	44
Table 3.10 The Effects Of Aging Temperature And Aging Time On The Microhardness Of AF1410 Steel	45

LIST OF FIGURES

	Page
Figure 2.1 Microstructure For The Longitudinal Orientation Of AF1410 Steel, 500X	7
Figure 2.2 Microstructure For The Transverse Orientation Of AF1410 Steel, 500X	8
Figure 2.3 Specimen Design For True Stress - True Strain Tensile Tests	11
Figure 2.4 Specimen Design For Elastic-Modulus Tests	13
Figure 2.5 Specimen Design For Stress-Relaxation Tests	14
Figure 2.6 The Relationship Between The Temperature Across A Specimen's Free Span And The type Of Tensile Test Jaw	15
Figure 3.1 The Ultimate Tensile Strength Of AF1410 Steel As A Function Of Temperature	23
Figure 3.2 The 0.1% Offset Yield Strength Of AF1410 Steel As A Function Of Temperature	24
Figure 3.3 The True Fracture Stress Of AF1410 Steel As A Function Of Temperature	25
Figure 3.4 The Reduction In Area Of AF1410 Steel As A Function Of Temperature	27
Figure 3.5 The True Fracture Strain Of AF1410 Steel As A Function Of Temperature	28
Figure 3.6 Young's Modulus Of AF1410 Steel As A Function Of Temperature	31
Figure 3.7 AF1410 Steel Stress-Relaxation Test Results For The Longitudinal Orientation	33
Figure 3.8 AF1410 Steel Stress-Relaxation Test Results For The Transverse Orientation ..	34
Figure 3.9 The Percent Stress Relaxation After One Hour As A Function Of Temperature	37

	Page
Figure 3.10 The 0.1% Offset Yield Strength For The Longitudinal Orientation Of As-Received And Aged AF1410 Steel As A Function Of Temperature	41
Figure 3.11 The 0.1% Offset Yield Strength For The Transverse Orientation Of As-Received And Aged AF1410 Steel As A Function Of Temperature	42
Figure 3.12 The Age-Hardening Response Of AF1410 Steel As A Function Of Temperature	46
Figure 3.13 The Age-Hardening Response Of AF1410 Steel As A Function Of Time	47
Figure 6.1 The GPL Program For Room-Temperature True Stress - True Strain Tensile Tests .	55
Figure 6.2 The GPL Program For True Stress - True Strain Tensile Tests Performed At 200°F .	57
Figure 6.3 The GPL Program For True Stress - True Strain Tensile Tests Performed At 400°F .	58
Figure 6.4 The GPL Program For True Stress - True Strain Tensile Tests Performed At 600°F .	59
Figure 6.5 The GPL Program For True Stress - True Strain Tensile Tests Performed At 800°F .	60
Figure 6.6 The GPL Program For Room-Temperature Elastic-Modulus Tensile Tests	61
Figure 6.7 The GPL Program For Elastic-Modulus Tensile Tests Performed At 200°F	62
Figure 6.8 The GPL Program For Elastic-Modulus Tensile Tests Performed At 400°F	63
Figure 6.9 The GPL Program For Elastic-Modulus Tensile Tests Performed At 600°F	64
Figure 6.10 The GPL Program For Elastic-Modulus Tensile Tests Performed At 800°F	65

ABSTRACT

The effect of thermal and mechanical transients on the material properties of AF1410 steel for applications in large caliber ballistic weapons was investigated. The Gleeble Model 1500 thermomechanical simulation device was used for the evaluation of elevated-temperature mechanical properties and simulated firing cycles. The tensile properties and the age-hardening response were measured, as a function of temperature, for one heat of AF1410 steel.

The results of the investigation showed that the ultimate tensile strength, yield strength, and true fracture stress decreased linearly with increasing temperature, up to 800°F. Young's modulus decreased with increasing temperature, while Poisson's ratio remained unchanged. The material exhibited stress relaxation at elevated temperatures, but not at room temperature, when loaded to 80% of its yield strength. It was found that the yield strength increased when the material had been previously aged at the same temperature.

The age-hardening response of the material exhibited a secondary hardening peak at approximately 900°F. The room-temperature hardness increased with increasing aging temperature up to the secondary hardening peak. A rapid decrease in the room-temperature hardness with increasing aging time occurred at 1000°F.

PART 1
INTRODUCTION

The selection of materials for modern military structural components is based on traditional design and economic considerations, as well as new demands for superior material properties. Not only must a material lend itself to fabrication at an acceptable cost and provide the required strength, but it must also insure a predictable service life even in the presence of a flaw or defect.

AF1410 (14wt% Co, 10wt% Ni) steel was developed, under Air Force sponsorship, for structural applications where a component will be loaded to near its yield strength to meet requirements of structural efficiency and economy. AF1410 steel combines high strength with superior fracture toughness and stress-corrosion resistance. The alloying addition of ten percent nickel and the subsequent heat treatment are primarily responsible for the relatively high strength and excellent fracture toughness. The alloy is strengthened during tempering by carbide precipitation, not by the formation of intermetallic compounds. Cobalt, added to maintain a high austenite-to-martensite transformation temperature, limits the amount of retained austenite in the steel after

quenching. The low carbon content (0.15wt%) of this alloy enables the material to be fabricated easily. Furthermore, the alloy has good hot and cold-working characteristics and is readily machined.

The high yield strength of AF1410 allows for the modification of a structural design to achieve increased weight efficiency. It is therefore of interest to investigate the effect of thermal cycling on the material properties of AF1410.

PART 2
MATERIALS AND PROCEDURE

A. Characterization Of Base Material

The chemical composition of the AF1410 steel used in this investigation, based on data obtained from Universal-Cyclops Specialty Steel Division, is shown in Table 2.1. The chemical composition of this heat of AF1410 steel appears to be well within the nominal values listed in Table 2.1.

The material was forged to dimensional tolerances set by Watervliet Arsenal/Benet Laboratories. A double austenitization and age heat treatment was used to develop maximum toughness and high strength in the AF1410 steel. A subzero treatment was used to assure minimum retained austenite (less than 1%). The specific heat treatment is given below:

1650°F (898°C): 1 hour at temperature - oil quench
1525°F (829°C): 1 hour at temperature - oil quench
-100°F (-73°C): 1 hour at temperature - air warm
950°F (510°C): 5 hours at temperature - oil quench

The fundamental room-temperature mechanical

TABLE 2.1

Chemical Analysis Of AF1410 Steel
Used In This Investigation (in weight percent).

<u>Element</u>	<u>Heat Analysis</u>	<u>Nominal</u> ^a
Carbon.....	0.16	0.13-0.17
Manganese.....	0.02	0.10
Silicon.....	0.03	0.10
Sulfur.....	0.001	0.005
Phosphorus.....	0.004	0.008
Chromium.....	1.94	2.0
Nickel.....	10.20	9.5-10.5
Cobalt.....	13.70	13.5-14.5
Molybdenum.....	1.02	0.9-1.1
Titanium.....	0.013	0.015
Aluminum.....	0.002	0.015
Oxygen.....	0.0019	-----
Nitrogen.....	0.0004	-----
Iron.....	Balance	

a. Single values are maximums.

properties for this alloy from the same heat, also supplied by Universal-Cyclops, are listed in Table 2.2.

Specimens used in this investigation were cut to a specific specimen geometry (a detailed discussion of the specimen design will be provided later in this section). Elevated-temperature tensile properties were measured for two material orientations: longitudinal direction (parallel to the forging direction) and transverse direction (perpendicular to the forging direction). Several small samples of AF1410 steel were sectioned for metallographic evaluation. Samples of both longitudinal and transverse orientations were prepared in order to examine for directionality of the microstructure. Inspection of samples in the as-polished condition revealed a very low inclusion content with no preferred orientation. Photomicrographs of longitudinal and transverse samples etched to reveal microstructural details are shown in Figures 2.1 and 2.2, respectively. The microstructure is that of tempered martensite with small amounts of retained austenite. The macrohardness (HRC or Rockwell "C" hardness) and microhardness (HV or Vickers hardness) of both orientations were measured. The measured hardness values were HRC 48 and HV₁₀₀₀ 481, and were found to be approximately equal for both longitudinal and transverse orientations.

TABLE 2.2
Fundamental Room-Temperature Mechanical Properties
Of AF1410 Steel Used In This Investigation.

TENSILE PROPERTIES ^a				FRACTURE TOUGHNESS ^b	
UTS	0.2% YS	Elong.	%RA	K_{IC}	K_Q
(KSI)	(KSI)	(%)	(%)	($KS\sqrt{in}$)	($KS\sqrt{in}$)
244	223	15.4	69.5	159	200

a. Average of eight tests.

b. K_{IC} is the result of one test, K_Q is the average of three tests.

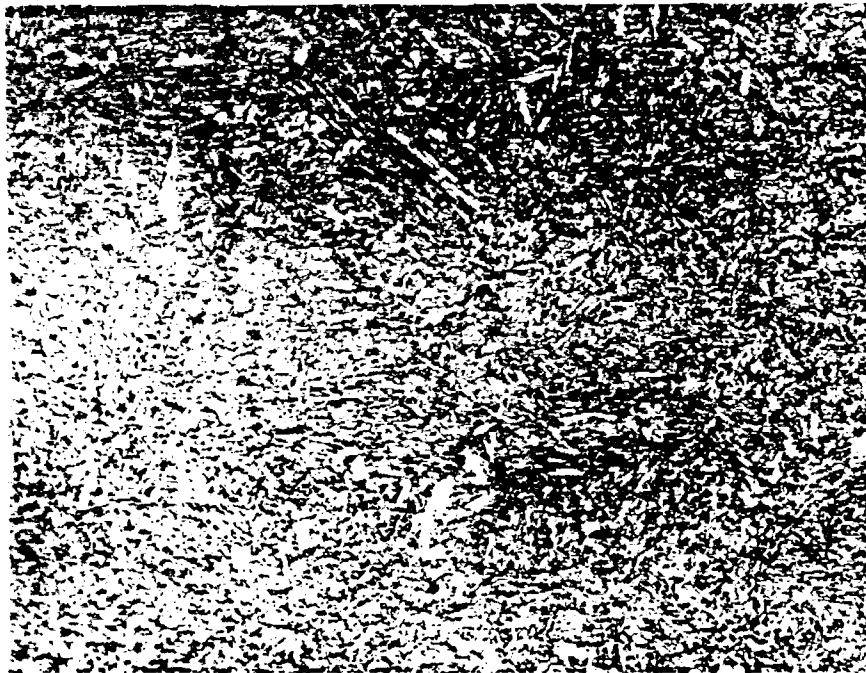


Figure 2.1 Microstructure For The Longitudinal
Orientation Of AF1410 Steel, 500X.

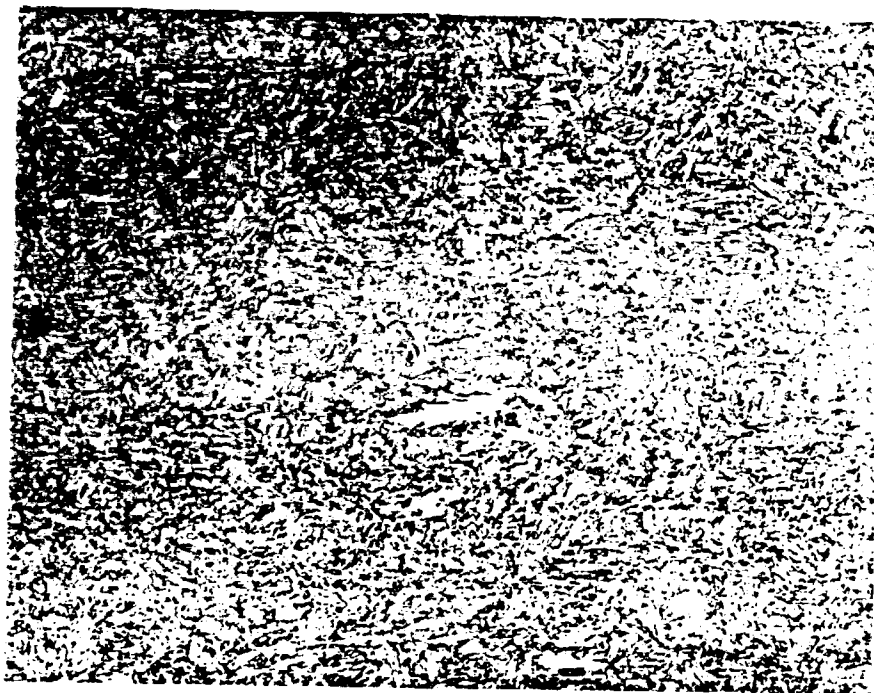


Figure 2.2 Microstructure For The Transverse
Orientation Of AF1410 Steel, 500X.

B. Tensile Testing

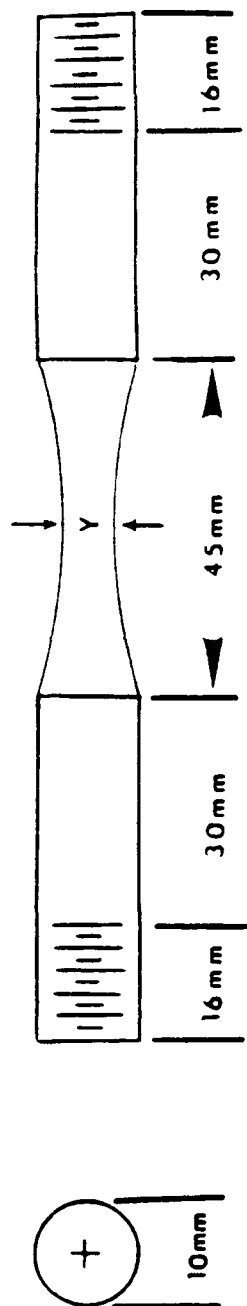
Tensile-test results in this investigation were generated using the Gleeble 1500, a thermomechanical simulation device. For elevated-temperature tests, the Gleeble 1500 utilizes controlled resistance heating. The specimen is clamped between two copper jaws and a two-wire, chromel-alumel thermocouple, condenser-discharge welded to the specimen at its midspan, provides for temperature measurement and control. In resistance heating, the maximum specimen temperature occurs at the midpoint between the two copper jaws (the specimen midspan). Because the jaws remain at ambient temperature, there is a temperature gradient along the specimen axis. The magnitude of this axial temperature gradient is a function of the jaw separation, thermal conductivities of the jaw and the specimen materials, and the maximum (control) temperature. The "hot" gage length is the effective gage length in a Gleeble test, and this value must be known for calculation of the strain rate.

True Stress - True Strain Tests

Given the secondary hardening response of AF1410 steel (References 1,2, and 3), the potential exists for

material at an elevated temperature (at the specimen midspan) to be stronger than material at a lower temperature down the axial temperature gradient. Therefore, a tensile failure in a resistance-heated specimen of uniform cross-section could occur at a location remote from the thermocouple, i.e., at an unknown temperature. For this reason, a continuous-radius gage length specimen was designed for this investigation. This specimen design, shown in Figure 2.3, should permit tensile testing at any temperature, including room temperature. Additionally, this specimen geometry will promote fracture at the specimen midspan so that a diametral dilatometer can be used for strain measurement.

The ultimate tensile strength (UTS), 0.1% offset yield strength (YS), percent reduction in area (%RA), true fracture stress, and true fracture strain, of AF1410 steel were determined using the true stress - true strain tensile test. A cross-head stroke rate of 0.675 cm/min was used and the specimen was pulled until failure. The GPL (Gleeble Programing Language) programs which generated the tensile test for the following temperatures: R.T., 200°F, 400°F, 600°F, and 800°F are shown in Figures 6.1-6.5 of the Appendix. Specimens were brought up to temperature in ten seconds and held there for thirty seconds prior to stroke movement. The tensile load, true



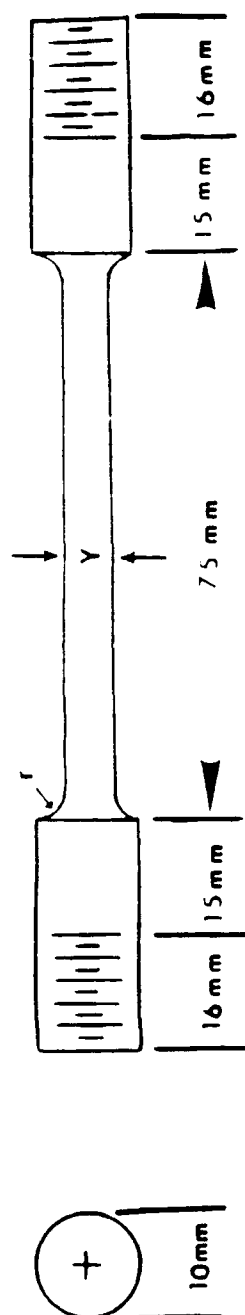
$$Y = 5 \text{ mm}$$

Figure 2.3 Specimen Design For True Stress - True Strain Tensile Tests.

stress, and true strain were recorded on an X-Y chart recorder. The UTS, YS, and true fracture stress were determined from these data. The %RA and true fracture strain were determined by optical measurements of the fracture surfaces of the tensile specimens.

Elastic-Modulus And Stress-Relaxation Tests

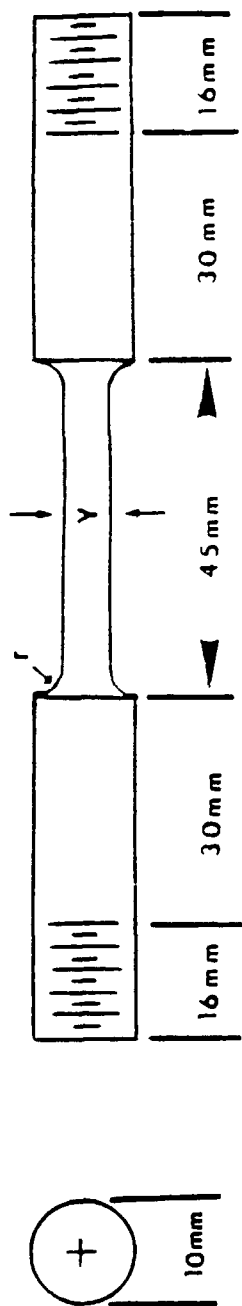
The determination of the elastic modulus and stress relaxation of a material requires a specimen with a uniform cross-section gage length (these tests are performed in the elastic region which eliminates the need for the continuous-radius gage length). The specimen configurations for elastic-modulus and stress-relaxation determination are shown in Figures 2.4 and 2.5, respectively. Both tests require small thermal gradients and longer work zones ("hot" gage lengths) to obtain more accurate results for the given test temperature. As has been discussed earlier, the thermal gradient can be reduced by increasing the length of the free span or by increasing the end temperature of the specimen. Hence hot jaws were used, where the temperature of the specimen end was increased by using a jaw with a lower thermal conductivity (stainless steel). The relationship between the temperature across the free span and the type of jaw used is shown in Figure 2.6 (Reference 4).



Y = 5mm

 $r = 5 \text{ mm}$

Figure 2.4 Specimen Design For Elastic-Modulus Tests.



$$Y = 5 \text{ mm}$$
$$r = 5 \text{ mm}$$

Figure 2.5 Specimen Design For Stress-Relaxation Tests.

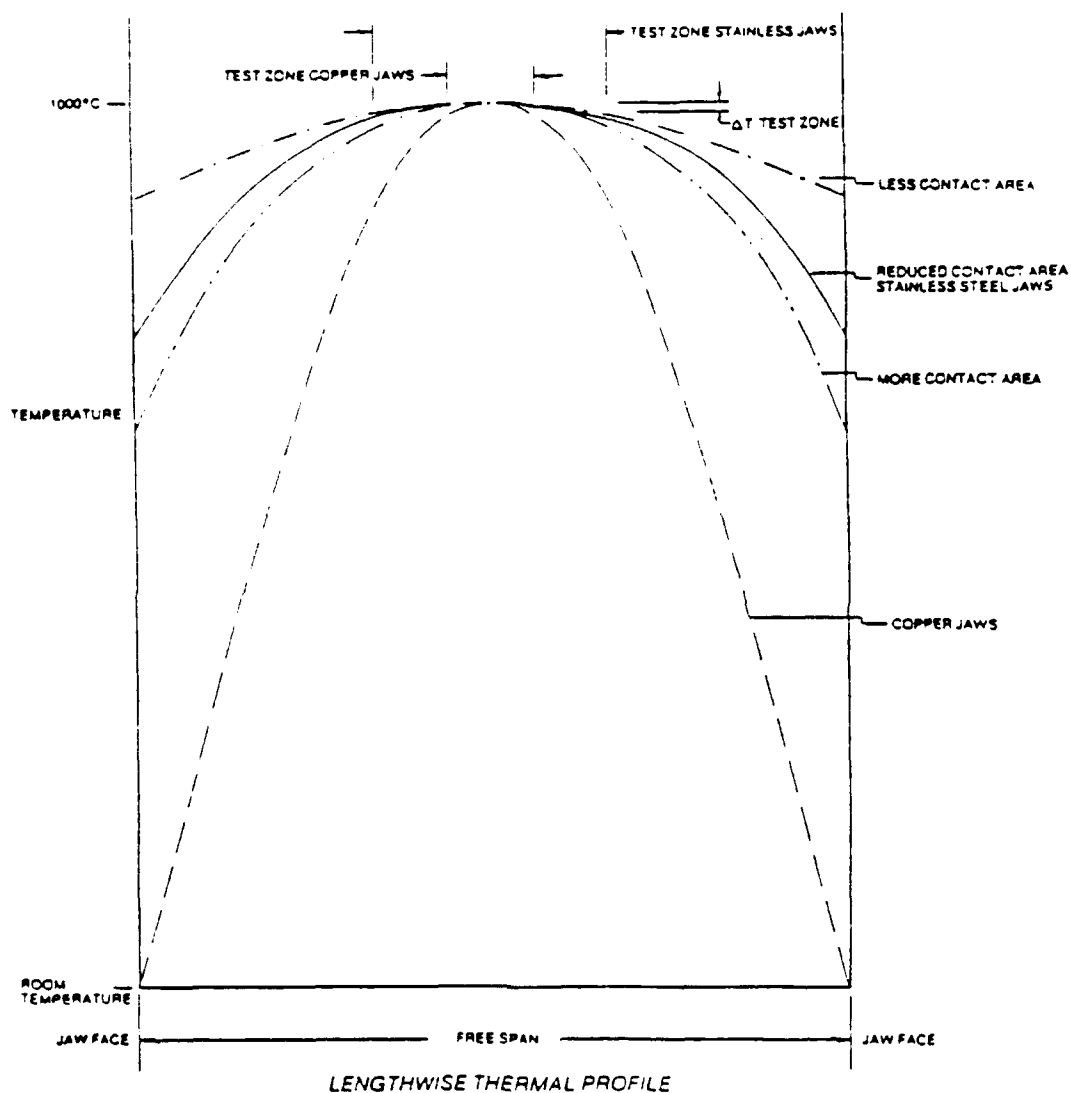


Figure 2.6 The Relationship Between The Temperature Across A Specimen's Free Span And The Type Of Tensile Test Jaw.

The elastic modulus (E) of the steel was measured using the following procedure. The specimens were heated to temperature in 30 seconds, and then held at temperature for 30 seconds. The specimens were then loaded to 80% of the yield strength, for the given temperature (R.T., 200°F, 400°F, 600°F, and 800°F), in 60 seconds.

The load, true stress, change in specimen axial length, and change in specimen diameter were recorded on an X-Y chart recorder. These data were then used to calculate Young's modulus and Poisson's ratio. The GPL programs for these tests are shown in Figures 6.6-6.10 in the Appendix.

Determination of stress relaxation of the steel was measured using the following procedure. The Gleeble 1500 system was put in the operational mode three hours prior to testing to eliminate potential mechanical, thermal, and electrical drifts and transients that might occur during long testing times. Specimens were manually heated and loaded in order to avoid compressive stresses on the specimen because of thermal expansion of the material during heating. The hydraulic drift of the mechanical system was determined and entered in the test as a \pm percent error. The specimens were heated to temperature in approximately 10 seconds, and the specimen was allowed to equilibrate at temperature. Specimens were loaded to 80% of the yield strength, for the given

temperatures (R.T., 200°F, 400°F, 600°F, and 800°F), in five seconds or less. The temperature and stroke position of the jaws were held constant for one hour. The load and stress of the specimens were recorded on a strip chart recorder and the percent stress relaxation after one hour was determined from these data.

Aging Tests

The specimens used in the stress-relaxation tests (held at temperature for one hour with an applied load) were unloaded and allowed to cool to room temperature in air. True stress - true strain tests were then performed on these stress-relaxation aged specimens. Specimens were tensile tested at the same temperature as those used in the stress-relaxation tests. The same testing procedure as that used previously in the true stress - true strain tests was used here, except that these specimens had a uniform cross-section gage length instead of a continuous-radius gage length.

C. Age-Hardening Response Testing

The properties of an age-hardenable alloy depend both on the temperature and the time of aging. In this investigation five test temperatures: 200°F, 400°F, 600°F, 800°F, and 1000°F, and five test times:

1/2hr, 1hr, 2hrs, 4hrs, and 6hrs, were chosen. Aging test specimens (1/2in x 5/16in x 1/8in) were cut from a section of the AF1410 forging. Specimens were aged in a Thermolyne 10500 Furnace. Each specimen was exposed to a different combination of time and temperature in order to form an experimental matrix. Specimens were placed in a fully preheated furnace and then air cooled outside the furnace at the completion of the aging treatment.

Specimens were ground through 600 grit emery to remove the oxide scale that had formed during aging. The room-temperature macrohardness, HRC or Rockwell "C" hardness, (150kg load, Brale indenter), of the aged specimens was determined using a Leco R-600 digital Rockwell hardness tester. Specimens were then mounted in bakelite and polished through 0.3-micron alumina using standard metallographic sample preparation. The room-temperature microhardness, HV or Vickers hardness (1kg load, equiaxed diamond pyramid indenter), of the aged specimens was determined using a Leco M-400 Vickers microhardness tester.

D. Metallography

All samples in this investigation were prepared for metallographic examination using standard techniques. Samples were embedded in 1.25in (31.75mm) diameter

bakelite mounts and prepared by successive stages of lapping, grinding, and mechanical polishing. Two levels of polishing were ordinarily used: 9-micron diamond abrasive on a cloth, and 0.3-micron alumina powder abrasive on a high-nap cloth. To prepare the sample for optical microscopy viewing, a 2% nital etchant was used. Photomicrography was performed using a Leco Neophot 21 metallograph and Polaroid type P/N 55 film.

PART 3

RESULTS AND DISCUSSION

A. Evaluation Of Tensile Tests

Tensile tests were performed on AF1410 steel at the following temperatures: R.T., 200°F, 400°F, 600°F, and 800°F. The tensile properties for the longitudinal and transverse orientations were determined from these tests.

True Stress - True Strain Tests

The tensile properties obtained from the true stress - true strain tensile tests, for the longitudinal and transverse orientations, are listed in Tables 3.1 and 3.2, respectively. These results were also plotted as a function of test temperature. The graphs for ultimate tensile strength (UTS), 0.1% offset yield strength (YS), and true fracture stress are shown in Figures 3.1, 3.2, and 3.3, respectively. These mechanical properties decreased linearly with increasing temperature. The lines contained in each of these figures are linear-regression fits. The results indicate that specimen orientation has little or no effect on the UTS, YS, and true fracture stress. The graphs for reduction in area (%RA) and true fracture strain are shown in Figures 3.4 and 3.5,

TABLE 3.1
Tensile Properties For The Longitudinal Orientation Of AF1410 Steel.

TEMPERATURE (°F)	%RA	UTS (KSI)	YS 0.1% (KSI)	TRUE FRACTURE STRESS (KSI)	TRUE FRACTURE STRAIN (in/in)	SPECIMEN NUMBER
RT	71.6	246	---	443	1.258	L-1
RT	70.6	244	194	406	1.225	L-2
RT	71.4	264	208	425	1.251	L-3
200	71.8	232	181	421	1.266	L-7
200	71.7	232	196	416	1.264	L-10
400	72.8	220	191	399	1.302	L-6
400	73.0	222	192	410	1.312	L-9
600	73.1	208	164	391	1.313	L-5
600	72.9	210	166	389	1.307	L-11
800	72.9	196	---	---	1.306	L-4
800	73.0	192	134	362	1.310	L-8

TABLE 3.2
Tensile Properties For The Transverse Orientation Of AF1410 Steel.

TEMPERATURE (°F)	%RA	UTS (KSI)	YS 0.1% (KSI)	TRUE FRACTURE STRESS (KSI)	TRUE FRACTURE STRAIN (in/in)	SPECIMEN NUMBER
RT	66.4	256	205	431	1.091	T-1
RT	66.9	251	207	416	1.106	T-9
RT	66.8	253	210	421	1.104	T-11
200	67.2	240	188	413	1.114	T-5
200	67.0	235	194	416	1.109	T-7
400	67.9	229	179	399	1.138	T-4
400	67.4	220	181	391	1.122	T-10
600	68.3	210	164	368	1.150	T-3
600	67.7	208	160	356	1.130	T-8
800	68.8	198	138	357	1.165	T-2
800	67.7	201	144	339	1.130	T-6

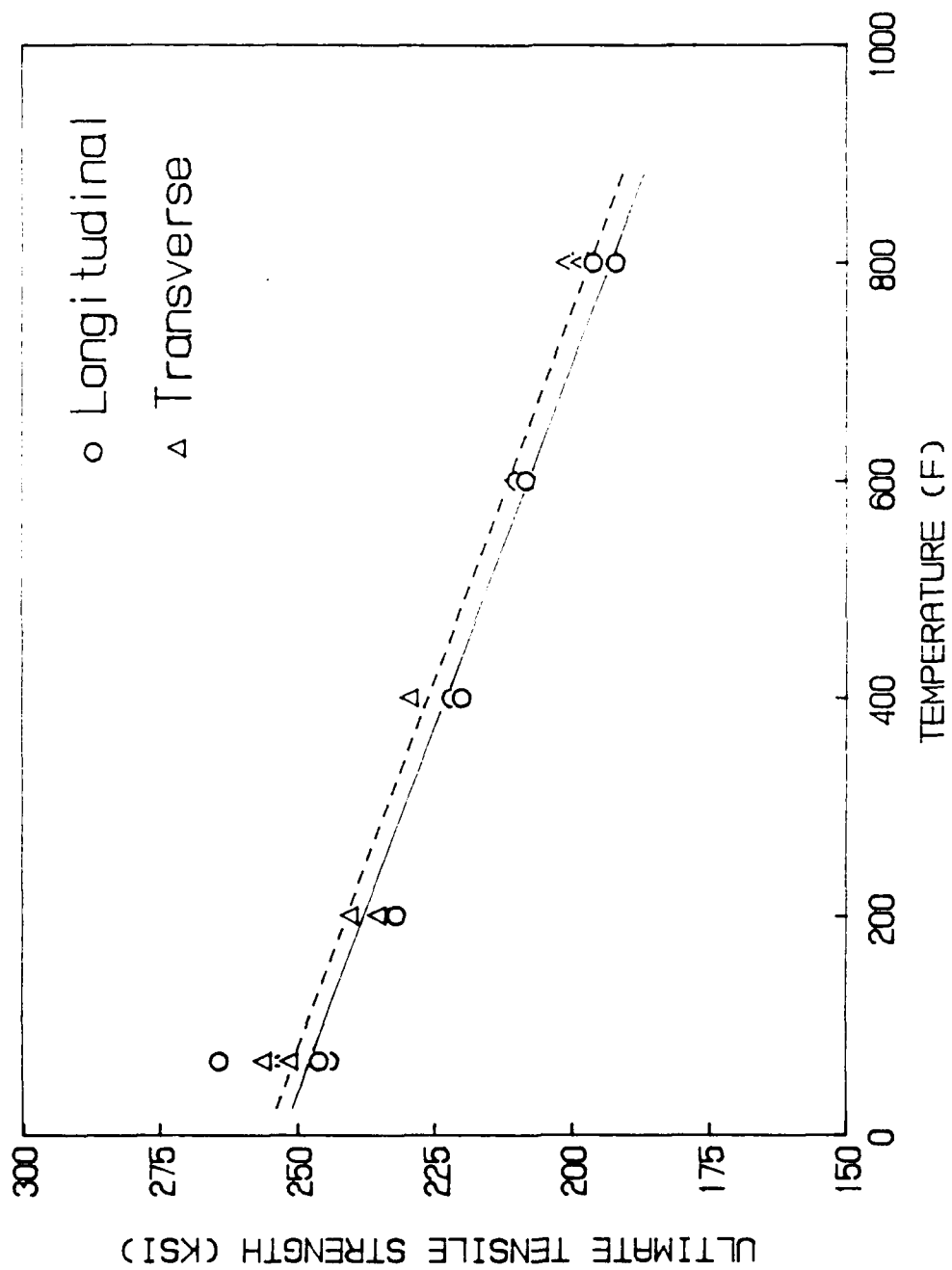


Figure 3.1 The Ultimate Tensile Strength of AF1410 Steel As A Function Of Temperature.

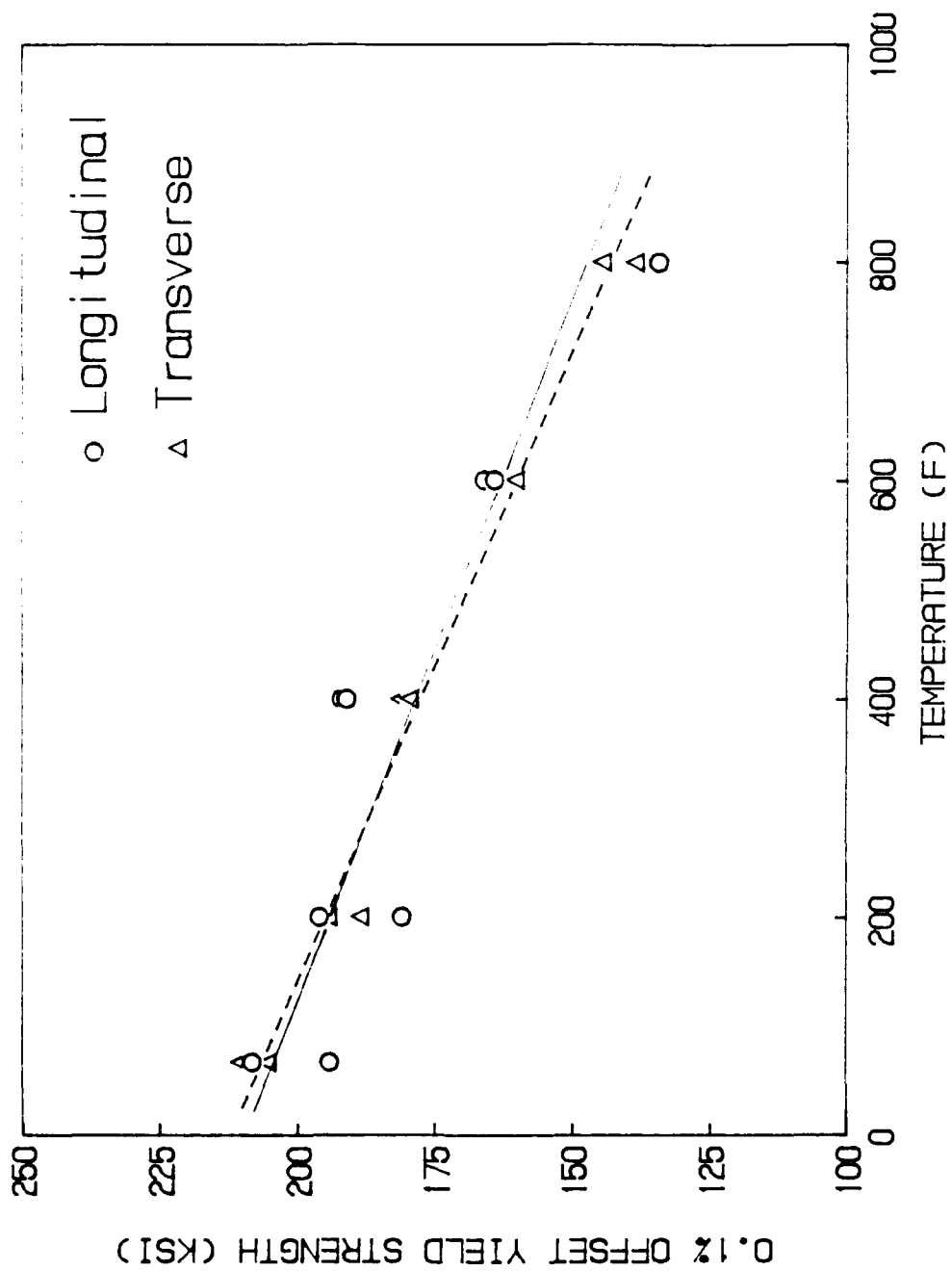


Figure 3.2 The 0.1% Offset Yield Strength of API 410 Steel As A Function Of Temperature.

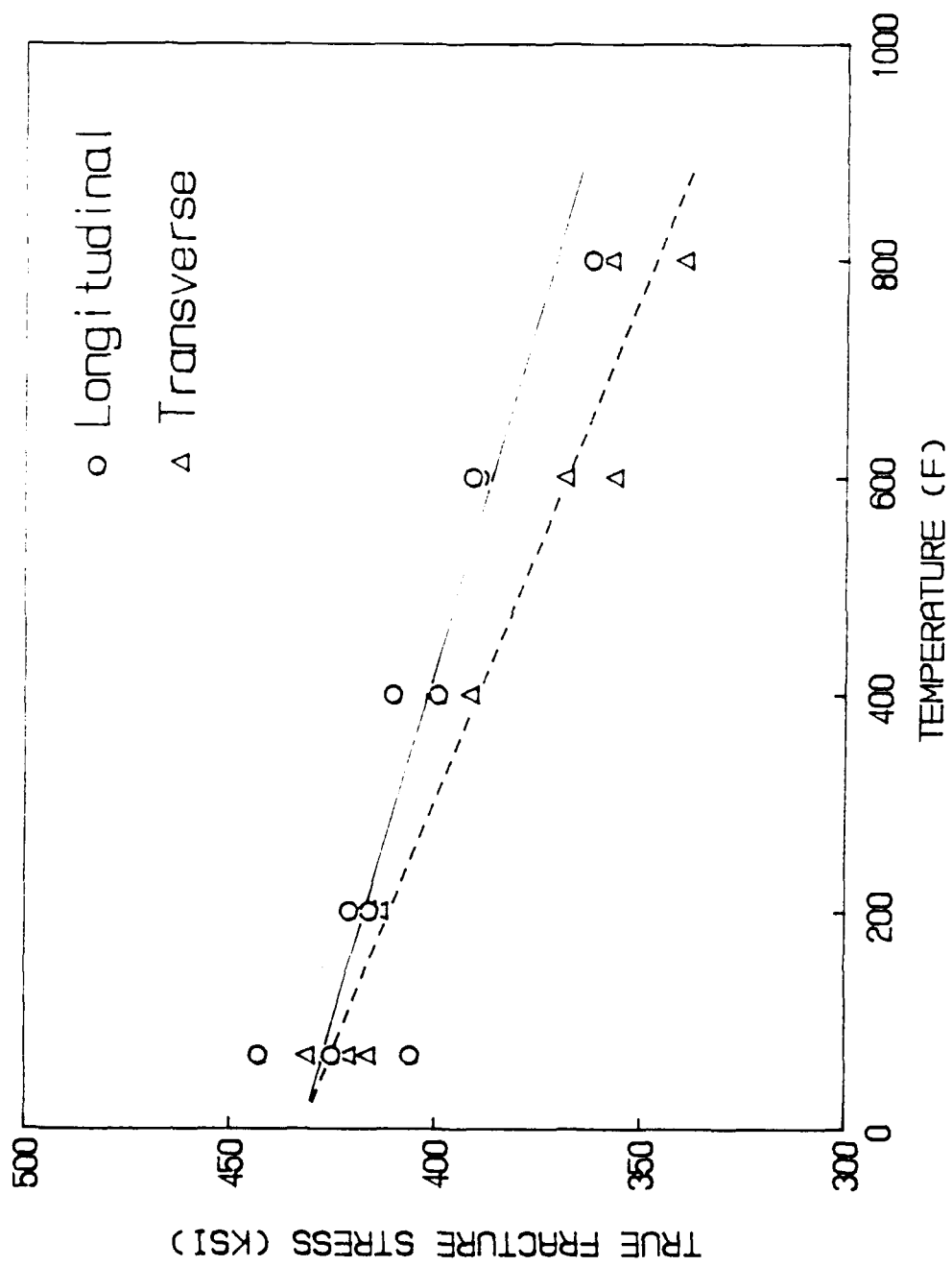


Figure 3.3 The True Fracture Stress of AFl410 Steel As A Function of Temperature.

respectively. The curves contained in each of these figures are second-order polynomial fits. The longitudinal specimen orientation exhibited a larger %RA and true fracture strain than the transverse specimen orientation for all of the test temperatures. The average percent difference in %RA and true fracture strain for the different orientations was determined to be approximately 7% and 13%, respectively. Both orientations did exhibit a similar increase in %RA and true fracture strain with increasing temperature. The rate at which the %RA and true fracture strain increased diminished as the temperature increased.

Elastic-Modulus And Stress-Relaxation Tests

Moduli of elasticity tests were performed on AF1410 steel for each test temperature. Young's moduli and Poisson's ratio results obtained for the longitudinal and transverse orientations are listed in Tables 3.3 and 3.4, respectively. The elastic moduli measurements at room temperature (68°F) compare favorably to the manufacturer's material specification of 29.4×10^3 Ksi. The Young's moduli results are shown graphically as a function of test temperature in Figure 3.6. The curves contained in the figure are second-order polynomial fits. Both specimen orientations exhibited a decrease in Young's

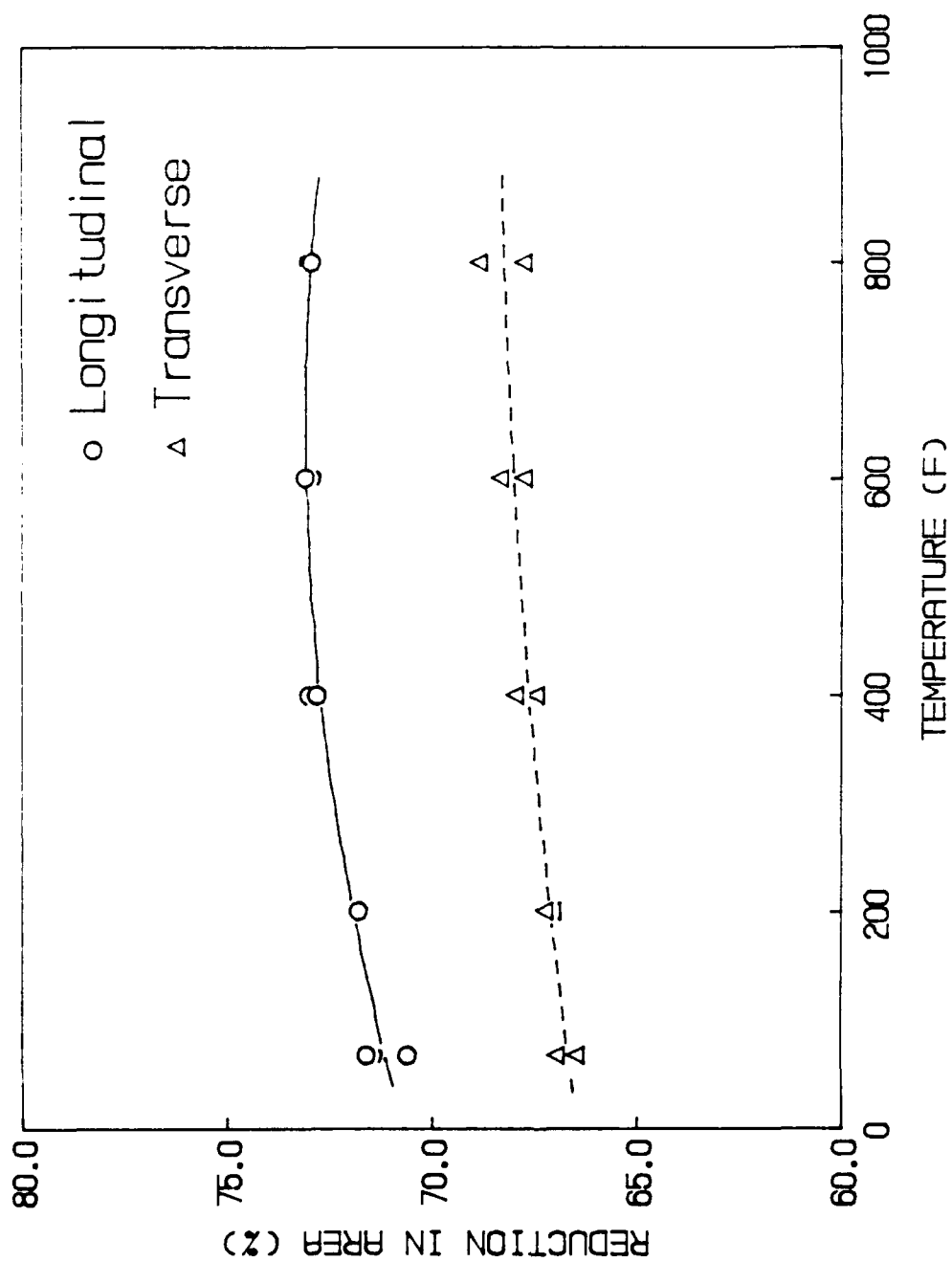


Figure 3.4 The Reduction In Area Of AF1410 Steel As A Function Of Temperature.

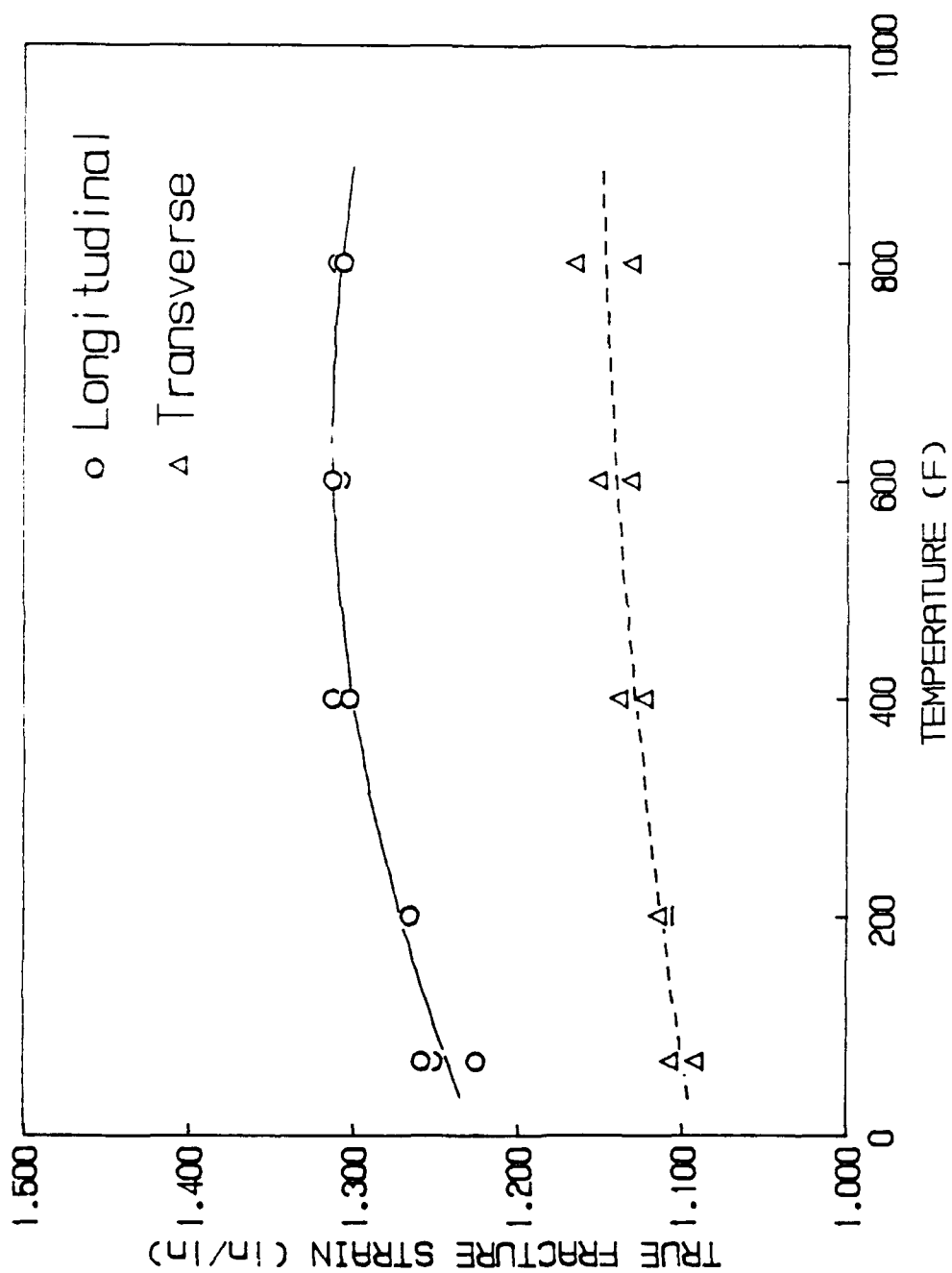


Figure 3.5 The True Fracture Strain of AF1410 Steel As A Function Of Temperature.

TABLE 3.3

Young's Modulus For The Longitudinal Orientation Of AF1410 Steel.

TEMPERATURE (°F)	YOUNG'S MODULUS (KSI)	POISSON'S RATIO	SPECIMEN NUMBER
RT	29,460	0.28	LM-1
RT	29,350	0.26	LM-2
200	29,280	0.27	LM-1
200	29,090	0.27	LM-2
400	28,810	0.27	LM-1
400	28,820	0.27	LM-2
600	28,630	0.27	LM-1
600	28,700	0.27	LM-2
800	27,610	0.27	LM-1
800	27,700	0.27	LM-2

TABLE 3.4
Young's Modulus For The Transverse Orientation Of AFl410 Steel.

TEMPERATURE (°F)	YOUNG'S MODULUS (KSI)	POISSON'S RATIO	SPECIMEN NUMBER
RT	28,620	0.26	TM-1
RT	28,610	0.27	TM-2
200	28,560	0.27	TM-1
200	28,440	0.26	TM-2
400	28,260	0.27	TM-1
400	27,900	0.26	TM-2
600	27,770	0.27	TM-1
600	27,510	0.27	TM-2
800	26,840	0.28	TM-1
800	26,720	0.27	TM-2

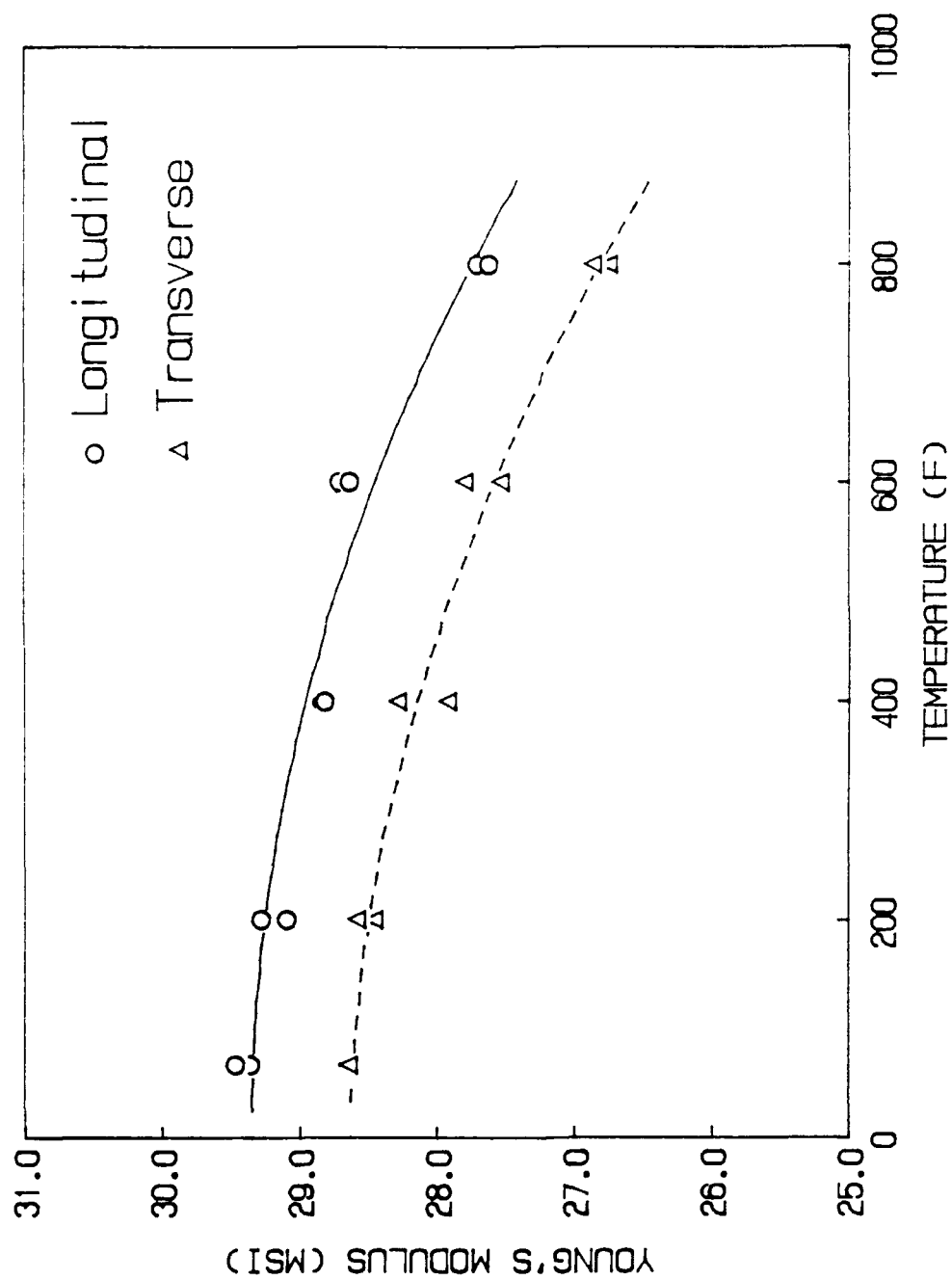


Figure 3.6 Young's Modulus of AFl410 Steel As A Function Of Temperature.

modulus with increasing temperature. The average percent difference in Young's modulus between the two orientations is less than 3%. The results of Poisson's ratio measurements display a small amount of scatter. It is believed that this scatter resulted from experimental error associated with the diametral dilatometer and axial extensometer, and therefore, the average measured value of Poisson's ratio, 0.27, is considered not to vary with temperature.

Results obtained for stress-relaxation tests performed on AF1410 steel in both the longitudinal and transverse orientations are presented in Figures 3.7 and 3.8, respectively. As the temperature is increased, the size of the specimen's hot gage length is decreased because of the increased axial thermal gradients. This difference in hot gage lengths is believed to have negligible influence on the stress-relaxation results because relaxation occurs predominantly at the hottest portion of the specimen. The values of percent stress relaxation after one hour obtained from these tests for the longitudinal and transverse orientations are listed in Tables 3.5 and 3.6, respectively. These values are also plotted as a function of test temperature in Figure 3.9. The lines contained in this figure are linear-regression fits and indicate that both orientations

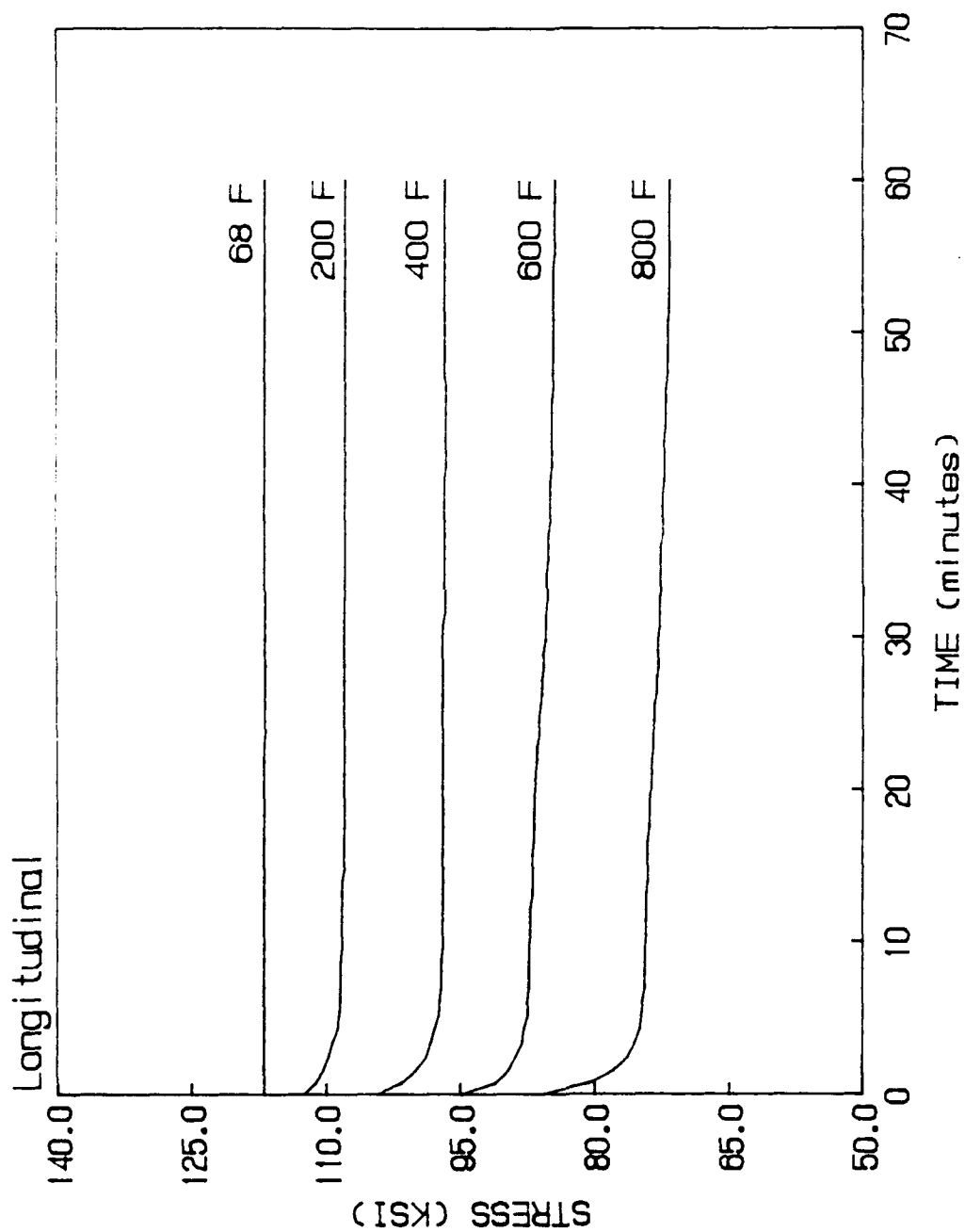


Figure 3.7 AF1410 Steel Stress-Relaxation Test Results For The Longitudinal Orientation.

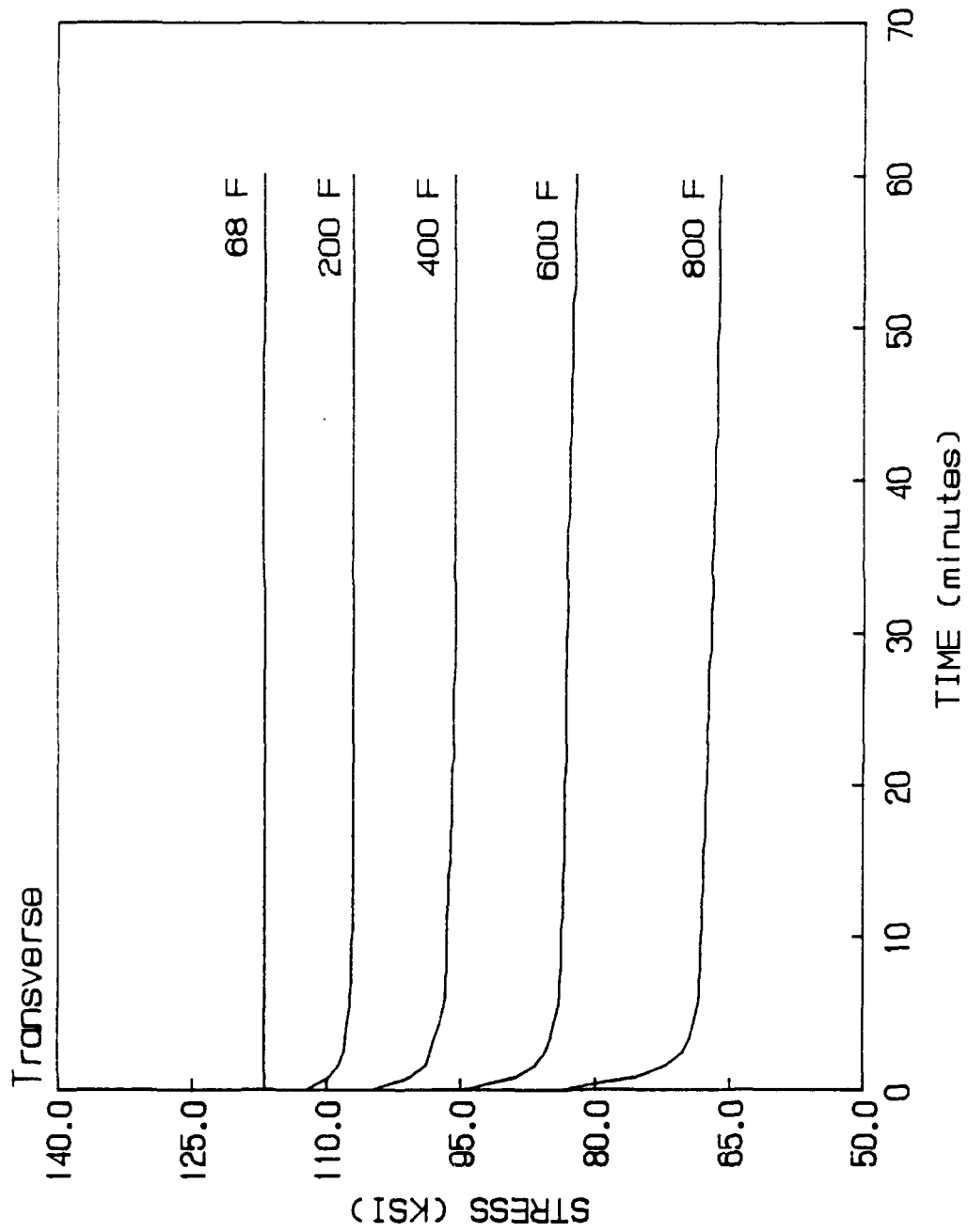


Figure 3.8 AF1410 Steel Stress-Relaxation Test Results For The Transverse Orientation.

TABLE 3.5
Stress Relaxation After One Hour
For The Longitudinal Orientation Of AF1410 Steel.

TEMPERATURE (°F)	INITIAL APPLIED STRESS OF 0.8YS (KSI)	STRESS RELAXATION AFTER ONE HOUR (PERCENT %)	SPECIMEN NUMBER
RT	166	0.51 ± 0.85	LSR-1
RT	166	0.00 ± 0.85	LSR-2
200	160	4.27 ± 0.89	LSR-4
200	159	3.84 ± 0.89	LSR-8
400	148	7.12 ± 0.96	LSR-6
400	148	7.98 ± 0.96	LSR-10
600	134	9.52 ± 1.06	LSR-7
600	135	12.62 ± 1.05	LSR-9
800	125	15.80 ± 1.14	LSR-3
800	120	17.68 ± 1.19	LSR-5

TABLE 3.6
Stress Relaxation After One Hour
For The Transverse Orientation Of AF1410 Steel.

TEMPERATURE (°F)	INITIAL APPLIED STRESS OF 0.8YS (KSI)	STRESS RELAXATION AFTER ONE HOUR (PERCENT %)	SPECIMEN NUMBER
RT	166	0.00 ± 0.85	TSR-1
RT	166	0.00 ± 0.85	TSR-2
200	160	5.35 ± 0.89	TSR-4
200	159	3.75 ± 0.89	TSR-10
400	149	8.57 ± 0.96	TSR-3
400	149	8.91 ± 0.96	TSR-9
600	134	13.33 ± 1.06	TSR-6
600	134	13.02 ± 1.06	TSR-8
800	120	21.43 ± 1.19	TSR-5
800	119	20.86 ± 1.20	TSR-7

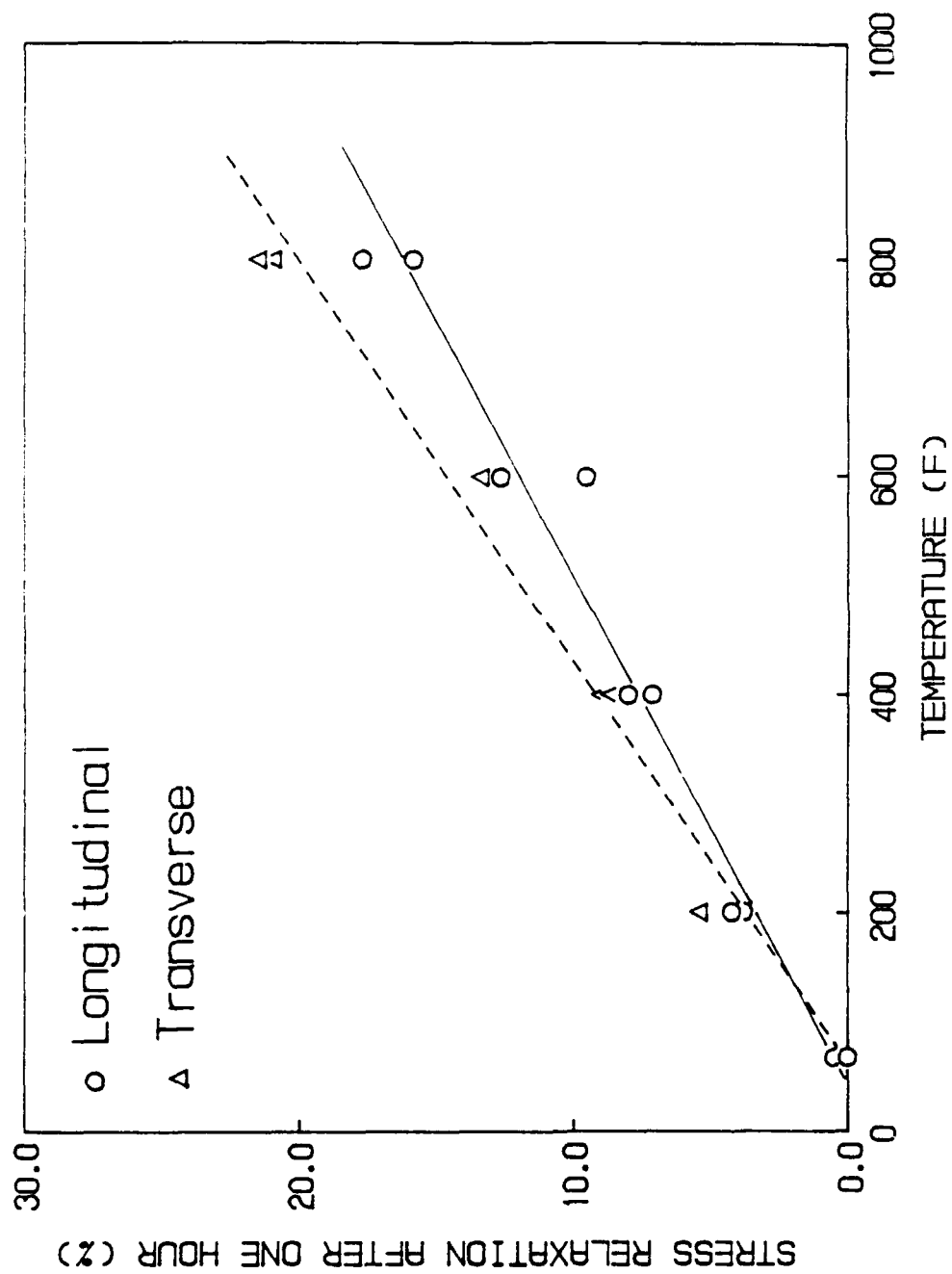


Figure 3.9 The Percent Stress Relaxation After One Hour As A Function Of Temperature.

exhibit approximately the same increase in stress relaxation with increasing temperature.

Aging Tests

True stress - true strain tensile tests were performed on the specimens used in the stress-relaxation tests. The data obtained from these tests for both the longitudinal and transverse orientations are listed in Tables 3.7 and 3.8, respectively. Because these specimens were previously held for one hour at the same temperature during stress-relaxation testing, these tensile properties will be referred to as being "aged". A comparison of the previously discussed tensile properties, Tables 3.1 and 3.2, to these aged tensile properties reveals a marked increase in the yield strength of the aged material with increasing aging temperature. This comparison of the yield strengths is shown graphically as a function of test temperature for both longitudinal and transverse orientations in Figures 3.10 and 3.11, respectively. The lines contained in each of these figures are linear-regression fits.

B. Evaluation Of Age-Hardening Response Tests

A brief study of the age-hardening response of AF1410 steel involved experiments at five aging

TABLE 3.7

Tensile Properties For The Longitudinal Orientation Of AF1410 Steel
That Were Previously Stress Relaxed At The Same Test Temperature.

TEMPERATURE (°F)	%RA	UTS (KSI)	YS 0.1% (KSI)	TRUE FRACTURE STRESS (KSI)	TRUE FRACTURE STRAIN (in/in)	SPECIMEN NUMBER
200	71.8	230	207	412	1.267	LSRL-4
200	72.5	230	202	415	1.290	LSRL-8
400	73.0	220	186	395	1.310	LSRL-6
400	72.9	221	184	393	1.305	LSRL-10
600	73.3	211	170	371	1.321	LSRL-7
600	73.0	205	168	380	1.310	LSRL-9
800	73.3	191	154	344	1.322	LSRL-3
800	73.3	195	158	356	1.322	LSRL-5

TABLE 3.8
Tensile Properties For The Transverse Orientation Of AFl410 Steel
That Were Previously Stress Relaxed At The Same Test Temperature.

TEMPERATURE (°F)	%RA	UTS (KSI)	YS 0.1% (KSI)	TRUE FRACTURE STRESS (KSI)	TRUE FRACTURE STRAIN (in/in)	SPECIMEN NUMBER
200	67.5	241	195	410	1.124	TSRT-4
200	67.0	236	192	402	1.108	TSRT-10
400	68.3	218	184	386	1.147	TSRT-3
400	67.9	222	184	393	1.139	TSRT-9
600	68.7	210	169	370	1.162	TSRT-6
600	68.5	206	171	381	1.156	TSRT-8
800	69.2	199	158	346	1.176	TSRT-5
800	68.9	199	159	352	1.168	TSRT-7

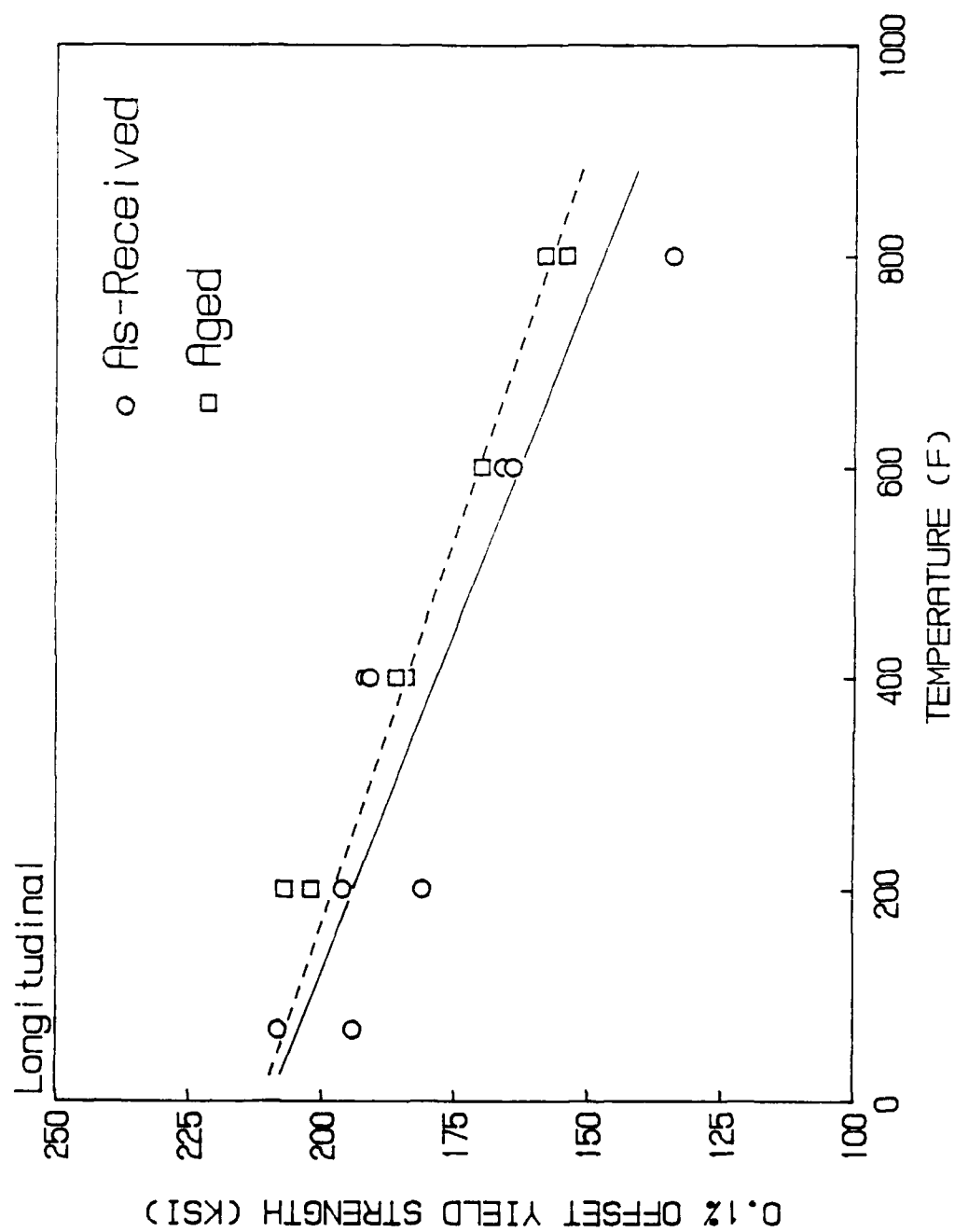


Figure 3.10 The 0.1% Offset Yield Strength For The Longitudinal Orientation Of As-Received And Aged AF1410 Steel As A Function Of Temperature.

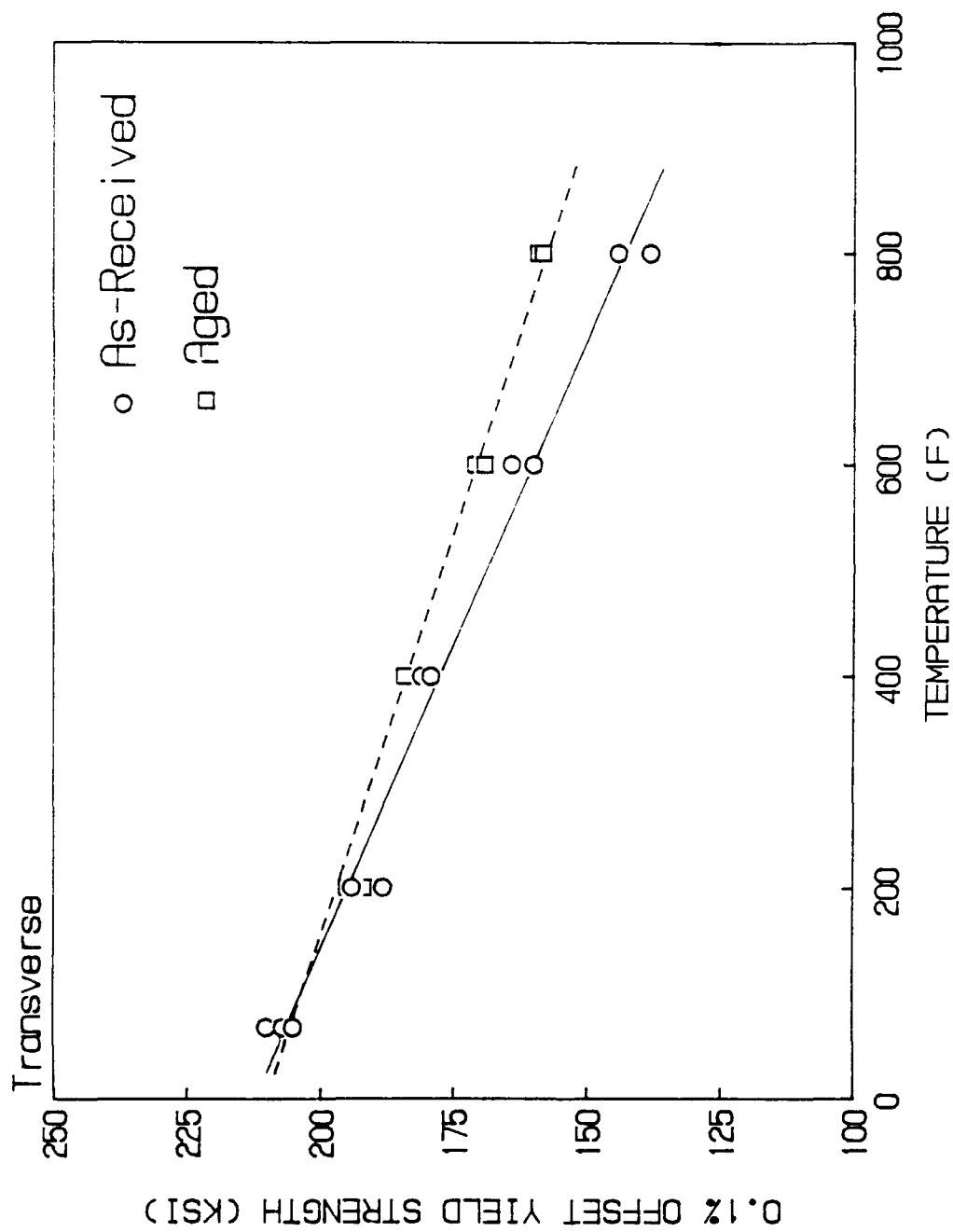


Figure 3.11 The 0.1% Offset Yield Strength For The Transverse Orientation Of As-Received And Aged AF1410 Steel As A Function Of Temperature.

temperatures and five aging times. Both macrohardness (HRC) and microhardness (HV_{1000}) tests were performed on the samples at room temperature. The macrohardness and microhardness results of the age-hardening tests are listed in Tables 3.9 and 3.10, respectively.

The age-hardening responses as a function of temperature and time are shown in Figures 3.12 and 3.13, respectively. The first sign of an increase in hardness was seen at 400°F, (Figure 3.12). At this aging temperature, Fe_3C has been reported to exist in an Fe-9Ni-4Co-0.4C steel (Reference 5). The carbide precipitation occurring in AF1410 steel at this temperature is mainly cementite. Investigations by Speich (Reference 6) demonstrate that the fine cementite precipitation forms at the grain and lath boundaries.

Progressively higher aging temperatures lead to coarsening of the boundary carbides (Reference 7). Between 800°F and 1000°F a secondary-hardening peak is formed, (Figure 3.12). Typical electron-transmission micrographs of Fe-10Ni-8Co-2Cr-1Mo steels (Reference 8), indicate that the coarse carbides are dissolving in this temperature range. Also revealed by the same micrographs is the existence of a fine dislocation-nucleated carbide; aging for longer times results in complete replacement of the coarse carbide by the fine dislocation-nucleated

TABLE 3.9
The Effects Of Aging Temperature And Aging Time
On The Macrohardness Of AF1410 Steel.

	TIME (Hours)				
	1/2	1	2	4	6
T	:	:	:	:	:
E	:	:	:	:	:
M	:	47.9	48.0	48.0	48.0
P	:	:	:	:	:
E	:	:	:	:	:
R	:	48.0	48.0	48.1	48.2
A	:	:	:	:	:
T	:	48.1	48.2	48.2	48.3
U	:	:	:	:	:
R	:	:	:	:	:
E	:	48.1	48.2	48.3	48.8
(F)	:	:	:	:	:
	:	:	:	:	:
1000	47.1	46.6	45.9	44.4	43.3
	:	:	:	:	:

NOTE: Hardness is based on the Rockwell "C" Scale.
Material as-received has a HRC of 48.0.

TABLE 3.10

The Effects Of Aging Temperature And Aging Time
On The Microhardness Of AF1410 Steel.

		TIME (Hours)				
		1/2	1	2	4	6
T	200	481	481	481	481	481
E						
M						
P	400	481	481	481	482	483
E						
R						
A	600	482	483	484	486	487
T						
U						
R	800	483	485	489	492	496
E						
(F)	1000	466	456	447	435	424

NOTE: Hardness is based on the Vickers DPH Scale.
Material as-received has a HV₁₀₀₀ of 481.

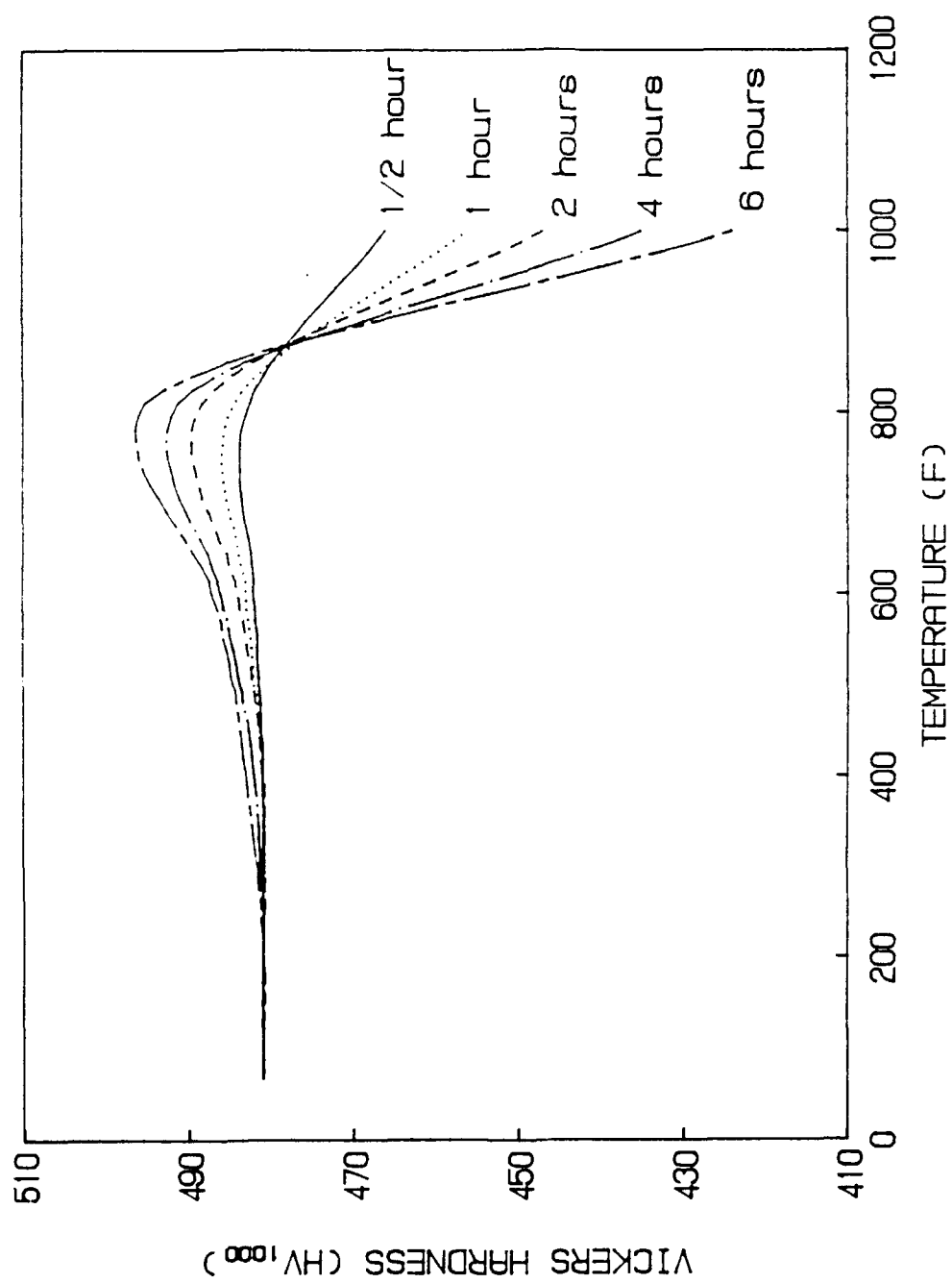


Figure 3.12 The Age-Hardening Response Of AF1410 Steel As A Function Of Temperature.

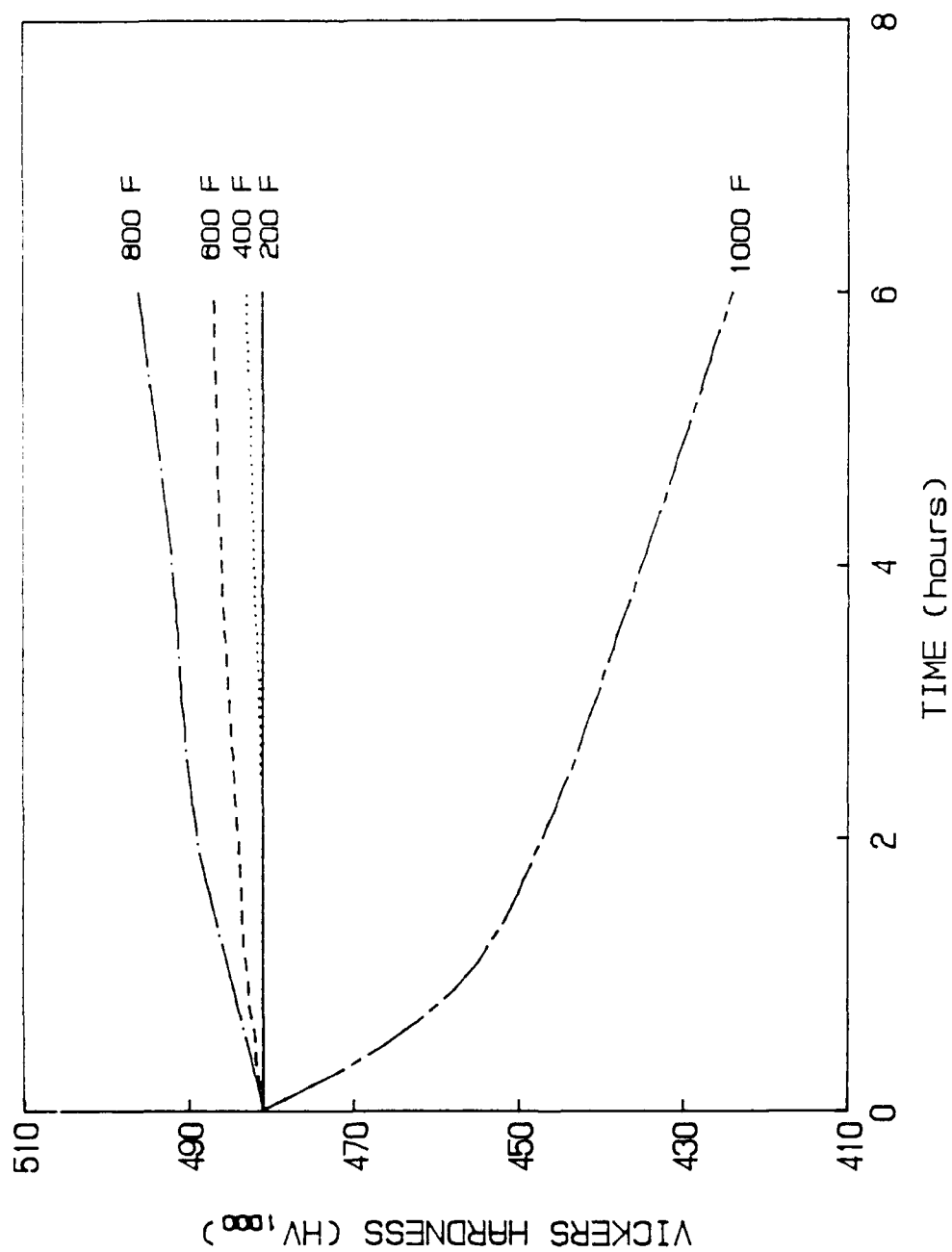


Figure 3.13 The Age-Hardening Response Of AF1410 Steel As A Function Of Time.

carbide. The dislocation-nucleated carbide coarsens gradually as the temperature is increased. A maximum age-hardening response results from an optimum carbide distribution, intercarbide spacing, and size of the dislocation-nucleated carbide precipitates.

The coarse cementite carbide is plate-like, while the fine dislocation-nucleated carbide, which is an Mo_2C -type carbide, is needle-like (Reference 9). Both of these carbides probably contain some other alloying elements in solid solution. Since Cr has a large effect upon the tempering kinetics of the Mo_2 -type carbide, it is believed the Mo_2C -type carbide contains large amounts of Cr and, therefore, should be referred to as $(\text{Mo}, \text{Cr})_2\text{C}$. Investigations by Krapf (Reference 10) on the precipitated phases in 10Ni maraging steel have indicated the existence of MoC , Mo_2C , Mo_xC , Fe_3C , Cr_7C_3 , and $(\text{Cr}, \text{Mo}) \text{C}_x$ type carbides over a wide range of aging times and temperatures.

It is believed that as the aging temperature is progressively increased above 900°C , the amount of reverted austenite present at room temperature will increase. In the aging temperature range of $900^\circ\text{--}950^\circ\text{F}$ the quantity of increased reverted austenite is thought to be small and primarily interlath. When overaged at 1000°F , a rapid decrease in hardness occurs,

(Figure 3.13). This rapid decrease in hardness is thought to be associated with the annealing of the dislocation substructure and an appreciable increase in the amount of reverted austenite, (Reference 1).

PART 4
CONCLUSIONS

The effect of elevated temperatures on the tensile properties of AF1410 steel was investigated. Specimens of this material were tensile tested at the following temperatures: R.T., 200°F, 400°F, 600°F, and 800°F. A brief experimental study of this material's age-hardening response at temperatures of 200°F, 400°F, 600°F, 800°F, and 1000°F was also included in this investigation. The primary findings of this investigation were:

1. The UTS, YS, and true fracture stress decreased linearly with increasing tensile test temperature. The orientation of the material exhibited little or no effect on these tensile properties.
2. The %RA and true fracture strain increased with increasing temperature. The rate at which these properties increased diminished with increasing temperature. The orientations had similar responses to increasing temperature, but the %RA and true fracture strain were consistently higher in the longitudinal direction than in the transverse direction.

3. Young's modulus decreased with increasing temperature. As the temperature increased, the modulus experienced a more rapid rate of decay.
4. At room temperature the material experienced no stress relaxation when initially loaded to 80% of the YS. At higher temperatures the percentage of stress relaxation increased with increasing temperature. The transverse orientation exhibited larger relaxations in stress than did the longitudinal orientation.
5. When the material was aged for one hour and then tensile tested at the aging temperature, the YS was higher than that of the as-received specimen tested at the same temperature. The largest difference between the as-received YS and the aged YS occurred at the maximum test temperature, 800°F.
6. Age-hardening response tests revealed that overaging takes place in the material in the range of 800°F to 1000°F. A maximum hardness was obtained after a 6-hour, 800°F treatment. The optically-viewed microstructure was not noticeably altered by the various aging treatments. It is believed that secondary-hardening takes place in this alloy when

iron carbides are replaced by alloyed carbides. It is proposed that annealing of the dislocation substructure, and an increase in the amount of reverted austenite are responsible for the rapid decrease in hardness when overaged at 1000°F.

PART 5
LITERATURE CITED

1. Machmeier, P.M.; DEVELOPMENT OF A WELDABLE HIGH STRENGTH STEEL; Technical Report AFML-TR-75-148, Sept. 1975.
2. Machmeier, P.M., Little, C.D., Horowitz, M.H., Oates, R.P.; DEVELOPMENT OF A STRONG (1650 MN/m² TENSILE STRENGTH) MARTENSITIC STEEL HAVING GOOD FRACTURE TOUGHNESS; Met. Technol. 6, (8), p.291-296, Aug. 1979.
3. Garrison, W.M. and Moody, N.R.; THE INFLUENCE OF INCLUSION SPACING AND MICROSTRUCTURE ON THE FRACTURE TOUGHNESS OF THE SECONDARY HARDENING STEEL AF1410; Met. Trans. 18A, p.1257-1263, Jul. 1987.
4. Duffers Scientific, Inc.; DYNAMIC THERMAL/MECHANICAL METALLURGY USING THE GLEEBLE 1500; user manual, 2nd edition, p.52.
5. Das, S.K. and Thomas, G.; STRUCTURE AND MECHANICAL PROPERTIES OF Fe-Ni-Co-C STEELS; Trans. ASM, vol. 62, p. 659, 1969.

6. Speich, G.R.; TEMPERING OF LOW-CARBON MARTENSITE;
Trans. of the Met. Society of AIME, Vol. 245,
p. 2553-64, 1969.
7. Giddings, J., Leak, G.M., and Nicholson, R.B.; THE
COARSENING BEHAVIOUR OF PURE IRON-CARBON ALLOYS;
Metal Science, Vol. 8, p. 349-52, 1974.
8. Speich, G.R., Dabkowski, D.S., and Porter, L.F.; STRENGTH
AND TOUGHNESS OF Fe-10Ni ALLOYS CONTAINING C, Cr, Mo,
AND Co; Met. Trans., Vol. 4, p. 303-15, 1973.
9. Hall, M.G., Kinsman, K.R., and Aaronson, H.I.; MECHANISM
OF FORMATION OF Mo₂C NEEDLES IN AN Fe-C-Mo ALLOY;
Met. Trans., Vol. 3, p. 1320-22, 1972.
10. Krapf, G.; INVESTIGATION OF PRECIPITATED PHASES IN 10Ni
MARAGING STEEL BY DTA-EGA TECHNIQUES AFTER VARIOUS
AGING TREATMENTS; JISI, p. 890-94, 1973.

PART 6

APPENDIX


```

PROGRAM : PEO      MECH RANGE = 0 - +10      April 21, 1989      14:47

PT.      TIME      TEMP      MODE      MECH      NO. OF      RETURN      CONTROL
          |         |         |         |         |         |         |         |
          |         |         |         |         |         |         |         |
0001      000:10.000  0000      SK         00.000      -----      -----      3, 4
0002      000:10.000  0000      SK         00.000      -----      -----      0, 1, 3, 4
0003      000:10.000  0000      SK         00.000      -----      -----      0, 1, 3, 4
0004      001:00.000  0000      SK         00.675      -----      -----      0, 1, 3, 4
0005      001:00.000  0000      SK         01.350      -----      -----      0, 1, 3, 4
0006      001:00.000  0000      SK         02.025      -----      -----      0, 1, 3, 4

```

Figure 6.1 The GPL Program For Room-Temperature True Stress - True Strain Tensile Tests.

PROGRAM : P93 MECH RANGE = 0 - +10 April 21, 1989 14:47

PT.	TIME	TEMP	MODE	MECH	NO. OF LOOPS	RETURN POINT	CONTROL SWITCHES ON
0001	000:10.000	0000	SK	00.000	----	----	2, 3, 4
0002	000:10.000	0000	SK	00.000	----	----	0, 1, 2, 3, 4
0003	000:10.000	0093	SK	00.000	----	----	0, 1, 2, 3, 4
0004	000:30.000	0093	SK	00.000	----	----	0, 1, 2, 3, 4
0005	001:00.000	0093	SK	00.675	----	----	0, 1, 2, 3, 4
0006	001:00.000	0093	SK	01.350	----	----	0, 1, 2, 3, 4
0007	001:00.000	0093	SK	02.025	----	----	0, 1, 2, 3, 4

Figure 6.2 The GPL Program For True Stress - True Strain Tensile Tests
Performed At 200°F.

PROGRAM : P204 MECH RANGE = 0 - +10 April 21, 1989 14:54

PT.	TIME	TEMP	MODE	MECH	NO. OF LOOPS	RETURN POINT	CONTROL SWITCHES ON
0001	000:10.000	0000	SK	00.000	----	----	2, 3, 4
0002	000:10.000	0000	SK	00.000	----	----	0, 1, 2, 3, 4
0003	000:10.000	0204	SK	00.000	----	----	0, 1, 2, 3, 4
0004	000:30.000	0204	SK	00.000	----	----	0, 1, 2, 3, 4
0005	001:00.000	0204	SK	00.675	----	----	0, 1, 2, 3, 4
0006	001:00.000	0204	SK	01.350	----	----	0, 1, 2, 3, 4
0007	001:00.000	0204	SK	02.025	----	----	0, 1, 2, 3, 4

Figure 6.3 The GPL Program For True Stress - True Strain Tensile Tests
Performed At 400°F.

PROGRAM : P316 MECH RANGE = 0 - +10 April 21, 1983 14:57

PT.	TIME	TEMP	MODE	MECH	NO. OF LOOPS	RETURN POINT	CONTROL SWITCHES ON
0001	000:10.000	0000	SK	00.000	----	----	2, 3, 4
0002	000:10.000	0000	SK	00.000	----	----	0, 1, 2, 3, 4
0003	000:10.000	0316	SK	00.000	----	----	0, 1, 2, 3, 4
0004	000:30.000	0316	SK	00.000	----	----	0, 1, 2, 3, 4
0005	001:00.000	0316	SK	00.675	----	----	0, 1, 2, 3, 4
0006	001:00.000	0316	SK	01.350	----	----	0, 1, 2, 3, 4
0007	001:00.000	0316	SK	02.025	----	----	0, 1, 2, 3, 4

Figure 6.4 The GPL Program For True Stress - True Strain Tensile Tests
 Performed At 600°F.

PROGRAM : P427 MECH RANGE = 0 - +10 April 21, 1989 14:58

PT.	TIME	TEMP	MODE	MECH	ND. OF LOOPS	RETURN POINT	CONTROL SWITCHES ON
0001	000:10.000	0000	SK	00.000	----	----	2, 3, 4
0002	000:10.000	0000	SK	00.000	----	----	0, 1, 2, 3, 4
0003	000:10.000	0427	SK	00.000	----	----	0, 1, 2, 3, 4
0004	000:30.000	0427	SK	00.000	----	----	0, 1, 2, 3, 4
0005	001:00.000	0427	SK	00.675	----	----	0, 1, 2, 3, 4
0006	001:00.000	0427	SK	01.350	----	----	0, 1, 2, 3, 4
0007	001:00.000	0427	SK	02.025	----	----	0, 1, 2, 3, 4

Figure 6.5 The GPL Program For True Stress - True Strain Tensile Tests
Performed At 800°F.

PROGRAM : E20 MECH RANGE = 0 - +10 April 21, 1989 14:58

PT.	TIME	TEMP	MODE	MECH	NO. OF LOOPS	RETURN POINT	CONTROL SWITCHES ON
0001	000:10.000	0000	FR	00.000	----	----	3
0002	000:10.000	0000	FR	00.000	----	----	0,1,3
0003	000:10.000	0000	FR	00.000	----	----	0,1,3
0004	001:00.000	0000	FR	02.250	----	----	0,1,3
0005	001:00.000	0000	FR	00.000	----	----	0,1,3

Figure 6.6 The GPL Program For Room-Temperature Elastic-Modulus Tensile Tests.

PROGRAM : E93 MECH RANGE = 0 - +10 April 21, 1989 14:59

PT.	TIME	TEMP	MODE	MECH	NO. OF LOOPS	RETURN POINT	CONTROL SWITCHES ON
0001	000:10.000	0000	FR	00.000	----	----	2, 3
0002	000:10.000	0000	FR	00.000	----	----	0, 1, 2, 3
0003	000:30.000	0093	FR	00.000	----	----	0, 1, 2, 3
0004	000:30.000	0093	FR	00.000	----	----	0, 1, 2, 3
0005	001:00.000	0093	FR	02.150	----	----	0, 1, 2, 3
0006	001:00.000	0093	FR	00.000	----	----	0, 1, 2, 3
0007	000:01.000	0020	FR	00.000	----	----	0, 1, 2, 3

Figure 6.7 The GPL Program For Elastic-Modulus Tensile Tests Performed
At 200°F.

PROGRAM : E204 MECH RANGE = 0 - +10 April 21, 1989 15:01

PT.	TIME	TEMP	MODE	MECH	NO. OF LOOPS	RETURN POINT	CONTROL SWITCHES ON
0001	000:10.000	0000	FR	00.000	----	----	2, 3
0002	000:10.000	0000	FR	00.000	----	----	0, 1, 2, 3
0003	000:30.000	0204	FR	00.000	----	----	0, 1, 2, 3
0004	000:30.000	0204	FR	00.000	----	----	0, 1, 2, 3
0005	001:00.000	0204	FR	02.000	----	----	0, 1, 2, 3
0006	001:00.000	0204	FR	00.000	----	----	0, 1, 2, 3
0007	000:01.000	0020	FR	00.000	----	----	0, 1, 2, 3

Figure 6.8 The GPL Program For Elastic-Modulus Tensile Tests Performed
At 400°F.


```

PROGRAM : E316      MECH RANGE = 0 - +10      April 21, 1989      15:01

PT.      TIME      TEMP      MODE      MECH      NO. OF      RETURN      CONTROL
          000:10.000  0000      FR      00.000    0000      0000      SWITCHES ON
0001      000:10.000  0000      FR      00.000    0000      0000      2, 3
0002      000:30.000  0315      FR      00.000    0000      0000      0, 1, 2, 3
0003      000:30.000  0315      FR      00.000    0000      0000      0, 1, 2, 3
0004      001:00.000  0315      FR      01.800    0000      0000      0, 1, 2, 3
0005      001:00.000  0315      FR      00.000    0000      0000      0, 1, 2, 3
0006      000:01.000  0020      FR      00.000    0000      0000      0, 1, 2, 3
0007

```

Figure 6.9 The GPL Program For Elastic-Modulus Tensile Tests Performed At 600°F.

PROGRAM : E427 MECH RANGE = 0 - +10 April 21, 1989 15:07

PT.	TIME	TEMP	MODE	MECH	NO. OF LOOPS	RETURN POINT	CONTROL SWITCHES ON
0001	000:10.000	0000	FR	00.000	----	----	2, 3
0002	000:10.000	0000	FR	00.000	----	----	0, 1, 2, 3
0003	000:10.000	0427	FR	00.000	----	----	0, 1, 2, 3
0004	000:30.000	0427	FR	00.000	----	----	0, 1, 2, 3
0005	001:00.000	0427	FR	01.500	----	----	0, 1, 2, 3
0006	001:00.000	0427	FR	00.000	----	----	0, 1, 2, 3
0007	000:01.000	0020	FR	00.000	----	----	0, 1, 2, 3

Figure 6.10 The GPL Program For Elastic-Modulus Tensile Tests Performed
At 800°F.

TECHNICAL REPORT INTERNAL DISTRIBUTION LIST

	NO. OF COPIES
CHIEF, DEVELOPMENT ENGINEERING DIVISION	
ATTN: SMCAR-CCB-D	1
-DA	1
-DC	1
-DI	1
-DP	1
-DR	1
-DS (SYSTEMS)	1
CHIEF, ENGINEERING SUPPORT DIVISION	
ATTN: SMCAR-CCB-S	1
-SE	1
CHIEF, RESEARCH DIVISION	
ATTN: SMCAR-CCB-R	2
-RA	1
-RE	1
-RM	1
-RP	1
-RT	1
TECHNICAL LIBRARY	5
ATTN: SMCAR-CCB-TL	
TECHNICAL PUBLICATIONS & EDITING SECTION	3
ATTN: SMCAR-CCB-TL	
OPERATIONS DIRECTORATE	1
ATTN: SMCWV-ODP-P	
DIRECTOR, PROCUREMENT DIRECTORATE	1
ATTN: SMCWV-PP	
DIRECTOR, PRODUCT ASSURANCE DIRECTORATE	1
ATTN: SMCWV-OA	

NOTE: PLEASE NOTIFY DIRECTOR, BENET LABORATORIES, ATTN: SMCAR-CCB-TL, OF ANY ADDRESS CHANGES.

TECHNICAL REPORT EXTERNAL DISTRIBUTION LIST

	<u>NO. OF COPIES</u>		<u>NO. OF COPIES</u>
ASST SEC OF THE ARMY RESEARCH AND DEVELOPMENT ATTN: DEPT FOR SCI AND TECH THE PENTAGON WASHINGTON, D.C. 20310-0103	1	COMMANDER ROCK ISLAND ARSENAL ATTN: SMCRI-ENM ROCK ISLAND, IL 61299-5000	1
ADMINISTRATOR DEFENSE TECHNICAL INFO CENTER ATTN: DTIC-FDAC CAMERON STATION ALEXANDRIA, VA 22304-6145	12	DIRECTOR US ARMY INDUSTRIAL BASE ENGR ACTV ATTN: AMXIB-P ROCK ISLAND, IL 61299-7260	1
COMMANDER US ARMY ARDEC ATTN: SMCAR-AEE	1	COMMANDER US ARMY TANK-AUTMV R&D COMMAND ATTN: AMSTA-DDL (TECH LIB) WARREN, MI 48397-5000	1
SMCAR-AES, BLDG. 321	1	COMMANDER	
SMCAR-AET-O, BLDG. 351N	1	US MILITARY ACADEMY	1
SMCAP-CC	1	ATTN: DEPARTMENT OF MECHANICS	
SMCAR-CCP-A	1	WEST POINT, NY 10996-1792	
SMCAR-FSA	1		
SMCAR-FSM-E	1	US ARMY MISSILE COMMAND	
SMCAR-FSS-D, BLDG. 94	1	REDSTONE SCIENTIFIC INFO CTR	2
SMCAR-IMI-I (STINFO) BLDG. 59	2	ATTN: DOCUMENTS SECT, BLDG. 4484	
PICATINNY ARSENAL, NJ 07806-5000		REDSTONE ARSENAL, AL 35898-5241	
DIRECTOR US ARMY BALLISTIC RESEARCH LABORATORY ATTN: SLCBR-DD-T, BLDG. 305 ABERDEEN PROVING GROUND, MD 21005-5066	1	COMMANDER US ARMY FGN SCIENCE AND TECH CTR ATTN: DRXST-SD 220 7TH STREET, N.E. CHARLOTTESVILLE, VA 22901	1
DIRECTOR US ARMY MATERIEL SYSTEMS ANALYSIS ACTV ATTN: AMXSY-MP ABERDEEN PROVING GROUND, MD 21005-5071	1	COMMANDER US ARMY LABCOM MATERIALS TECHNOLOGY LAB ATTN: SLCMT-IML (TECH LIB) WATERTOWN, MA 02172-0001	2
COMMANDER HQ, AMCCOM ATTN: AMSMC-IMP-L ROCK ISLAND, IL 61299-6000	1		

NOTE: PLEASE NOTIFY COMMANDER, ARMAMENT RESEARCH, DEVELOPMENT, AND ENGINEERING CENTER, US ARMY AMCCOM, ATTN: BENET LABORATORIES, SMCAR-CCB-TL, WATERVLIET, NY 12189-4050, OF ANY ADDRESS CHANGES.

TECHNICAL REPORT EXTERNAL DISTRIBUTION LIST (CONT'D)

	<u>NO. OF COPIES</u>		<u>NO. OF COPIES</u>
COMMANDER US ARMY LABCOM, ISA ATTN: SLCIS-IM-TL 2800 POWDER MILL ROAD ADELPHI, MD 20783-1145	1	COMMANDER AIR FORCE ARMAMENT LABORATORY ATTN: AFATL/MN EGLIN AFB, FL 32542-5434	1
COMMANDER US ARMY RESEARCH OFFICE ATTN: CHIEF, IPO P.O. BOX 12211 RESEARCH TRIANGLE PARK, NC 27709-2211	1	COMMANDER AIR FORCE ARMAMENT LABORATORY ATTN: AFATL/MNF EGLIN AFB, FL 32542-5434	1
DIRECTOR US NAVAL RESEARCH LAB ATTN: MATERIALS SCI & TECH DIVISION CODE 25-27 (DOC LIB) WASHINGTON, D.C. 20375	1 1	MIAC/CINDAS PURDUE UNIVERSITY 2595 YEAGER ROAD WEST LAFAYETTE, IN 47905	1
DIRECTOR US ARMY BALLISTIC RESEARCH LABORATORY ATTN: SLCBR-IB-M (DR. BRUCE BURNS) ABERDEEN PROVING GROUND, MD 21005-5066	1		

NOTE: PLEASE NOTIFY COMMANDER, ARMAMENT RESEARCH, DEVELOPMENT, AND ENGINEERING CENTER, US ARMY AMCCOM, ATTN: BENET LABORATORIES, SMCAR-CCB-TL, WATERVLIET, NY 12189-4050, OF ANY ADDRESS CHANGES.